Chemical insights into bioinks for 3D printing

Laurine Valot, Jean Martinez, Ahmad Mehdi, Gilles Subra

Chemical insights in bioinks for 3D printing

Laurine Valot,[a,b] Jean Martinez,[a] Ahmad Mehdi,[*b] and Gilles Subra[*a]

3D printing has triggered the acceleration of numerous research areas in health sciences, which traditionally used cells as starting materials, in particular tissue engineering, regenerative medicine but also in the design of more relevant bioassays for drug discovery and development. While cells can be successfully printed in 2D layers without the help of any supporting biomaterial, the obtainment of more complex 3D architectures requires a specific bioink, i.e. a material in which the cells are embedded during and after the printing process helping to support them while they are arranged in superimposed layers. The bioink plays a critical role in bioprinting: first, it must be adapted to the 3D printing technology, then, it must fulfil the physicochemical and mechanical characteristics of the target construct (e.g. stiffness, elasticity, robustness, transparency); finally it should guarantee cell viability and eventually induce a desired behaviour. This review focuses on the nature of the bioink components from natural or synthetic origin, and highlights the chemistry required for the establishment of the 3D network in conditions compatible with the selected 3D printing technique and cell survival.

Table of Contents

[a] Institute of Biomolecules Max Mousseron, UMR5247 CNRS, ENSCM, Université Montpellier, Faculté de Pharmacie 15 avenue Charles Flahault, 34093 Montpellier, France.

[b] Institute Charles Gerhardt, UMR5253 CNRS, ENSCM, Université Montpellier, Place Eugène Bataillon, 34095 Montpellier France.

*gilles.subra@umontpellier.fr and ahmad.mehdi@umontpellier.fr

1. Introduction

Supported by recent advances in 3D printing technology, researchers have explored new avenues for cell-based therapies and tissue engineering using cell encapsulated biomaterials. From a technical point of view, bioprinting is now feasible with a wide range of 3D printers, which are more and more affordable, reliable and easy-to-use, ranging from basic to sophisticated setups (more than one extruder, better resolution in deposition and thickness, etc.). Numerous inks are now readily available, meeting all the physical and chemical requirements for 3D printing on a particular device (e.g. extrusion, ink-jet, laser-based printer, etc.). Perhaps the simplest way to prepare cell-containing materials is first to print the scaffold, and seeding its surface with cells afterwards. Nevertheless, it is a much more challenging goal to design a bioink - i.e. an ink already encapsulating cells before printing. There are additional constraints for encapsulating cells from the beginning, guaranteeing their survival during the bioprinting process and guiding their behaviour once embedded in the final printed scaffold. On the other hand, 3D-bioprinting allows a homogeneous distribution of cells inside the construct and may yield more complex structures (e.g. for co-culture), compared to basic seeding on the surface of a printed scaffold. This major advantage is obtained at the cost of more restrictive 3D-printing procedures (no heating, no organic solvent, etc.) and the nature of the bioink, which can only be hydrogel.

Although there are many papers on these topics, neither 3D printing of cells alone suspended in culture medium or DPBS buffer (without any hydrogel support), nor works dealing with 3D printed objects seeded with cells, will be covered in this review. In the last 5 years, the number of publications on 3D printing has skyrocketed (Fig. 1), but only a small amount of them (less than 6%) really concerns bioprinting and only a minority of these articles describes a new bioink composition as most of the papers are focussed on new applications using well-known hydrogels (e.g. alginate, gelatin). Nevertheless, to mimic the biological complexity and the heterogeneity of natural tissues, it is important to have access to a wide range of different bioinks whose nature, physical and chemical properties can be chosen in accordance with the 3D printing method. This review focuses on bioink chemistry, which has already enabled the biofabrication of vessels,[1–3] tissues and skin,[4–9] cartilage[10–12] and bone.[13–16] Besides artificial organs,[17–21] the preparation of relevant 3D models[22–24] recapitulating the microenvironment of natural tissues has also been successfully performed by 3D bioprinting, in particular for screening of anticancer drugs and comprehension of tumour invasion mechanisms.[25–28] 3D biofabrication can also be merged with either improved drug delivery[29,30] by encapsulation of drugs inside the scaffold, or cell therapy.[31]

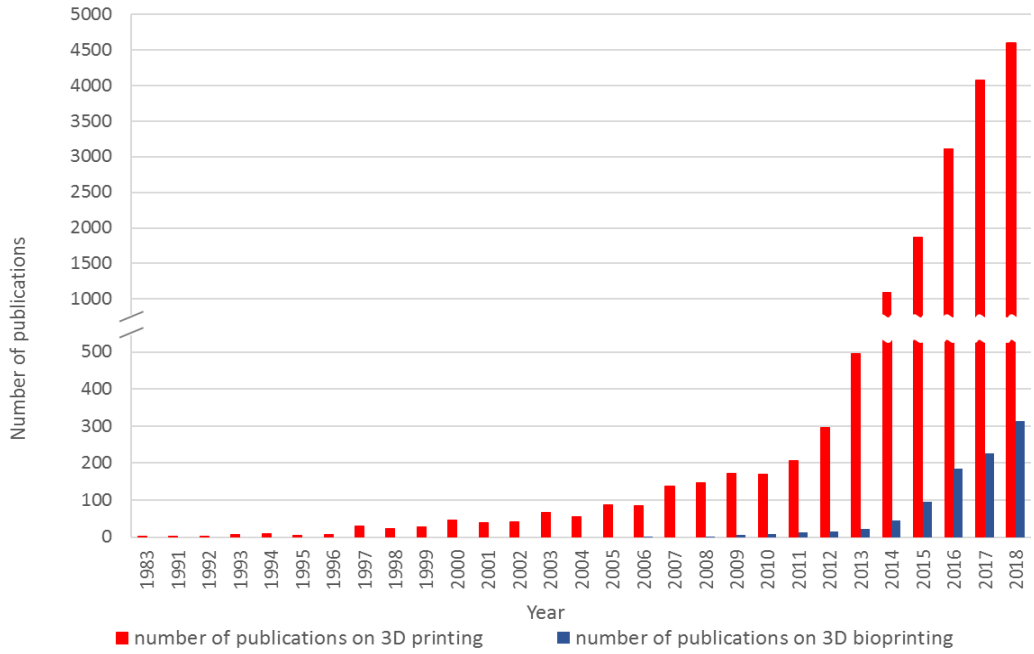

Fig. 1 Evolution of the number of publications by year on 3D printing (red) and on 3D-bioprinting (blue). Number of publications according to Web of Science from 1983 to 21st September 2018.

The nature of bioink is intimately associated with the different biocompatible 3D-printing technologies (Fig. 2), which are the topic of the following section. The chemical nature of bioink components [i.e. the (bio)polymers and building blocks used to establish the hydrogel network], and the chemical process leading to the cross-linking of the hydrogel will be discussed extensively in the third and fourth sections, respectively. Finally, we will try to ascertain what could next be contributed to the field of bioprinting by the creativity of organic, bioorganic or polymer chemists.

2. Biocompatible 3D-printing techniques: influence on bioink design

An obvious prerequisite to printing cells is to use a printer technique, which preserves the cell integrity during the 3D printing process. Fortunately, most of them are compatible with cell printing and cause only little trauma to the cells. Each technique is compatible with only some gelation processes (see 2.2-2.7 and chapter 4) and also requires inks that show specific mechanical and physical properties. Usually, it is the bioink that is adapted to the printer and not the other way round, mainly because of the cost of the apparatus (from $100 for the cheaper fused deposition modelling printers, $5000 for the simplest extrusion printer to one million dollars for a laser-based printer), even if a particularly attractive bioink can be assayed on different printers.[32] Big improvements have been made in 3D-printing technologies, offering new capabilities (such as multiple print-heads with different 3D printing technologies on the same printer) and better performance, for a lower cost by an ever growing number of manufacturers.[32] As obvious as it may seem it must be pointed out that 3D-bioprinting of big objects will always be limited by (i) the dimensions of the printer, (ii) the amount of bioink needed, and (iii) the size of the bioink reservoir. For further description of commercially available bio-printers, the reader can refer to a very complete review by Ozbolat *et al.*[32]

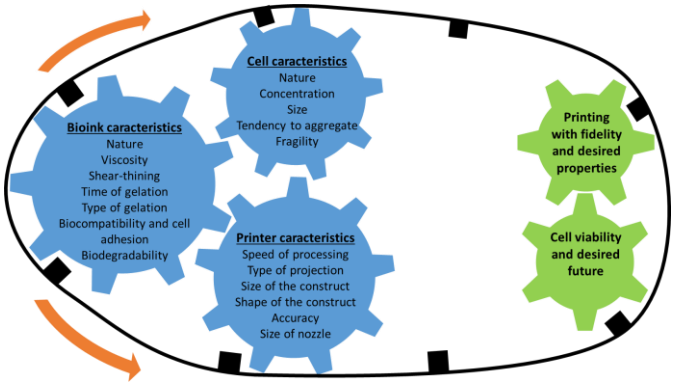

Fig. 2 Connexions between bioink characteristics, cells and printer.

2.1. Biological prerequisites for bioprinting

To print cells, a printing process must respect some rules linked to the gelation reaction and the ejection/shaping of the material. Obviously, temperature, pH, irradiation (UV, laser jetting, etc.) and pressure must be adapted to reduce cell mortality, considering that cell lines have different resistance to these parameters. Interestingly, compared to direct printing of cells alone, the embedding material (i.e. the bioink) may protect the cells for a limited time from exposure to lethal conditions (pressure, irradiation, etc.). However it is not advised to:

- Print above 50 °C or below 5 °C, otherwise it will induce cell death or growth retardation;
- Work at pH below 6.5 or above 7.8, because it will induce poor cell viability;[33]
- Use organic solvents or cytotoxic compounds (e.g. toxic catalysts, linkers, etc.). This means that only aqueous solutions can be bioprinted;
- Extrude with a high pressure (limits depend on cells and embedding material). As an example, when rat endothelial cells (RAMEC) suspended into an alginate hydrogel were extruded at 40 PSI, because of the effect of pressure, the survival rate fall to 60%.[34]

Moreover, conservation of cells in the ink prior to the printing process implies that the cell-embedded material follows basic sterility rules to avoid any bacteria or fungi contaminations. The bioink material needs to be prepared in sterile conditions or sterilised. It can be done by:

- Filtration if it is liquid enough, with a 0.22 µm filter,
- UV irradiation for a transparent solution or hydrogel, but only if it cannot undergo unwanted UV-crosslinking reactions,
- Autoclaving, only for compounds and solutions that are stable at high temperature, high pressure and humidity (i.e. up to 130°C with a humidity saturated atmosphere).

Of course once the cells are added to the bioink solution, the subsequent steps of the preparation of bioink (e.g. filling the reservoir, preliminary cross-linking), the printing process, and after-printing treatments must be performed under a sterile hood. It is worth noting that most 3D printers are small enough to fit inside a sterile hood thus easily complying with sterility requirements. The design of some other bioprinters include a sterile hood (e.g. Biofactory and 3DDiscovery from Regen Hu, Bio X and Inkredible + from Cellink, and 3Dn-300-TE from nScrypt).

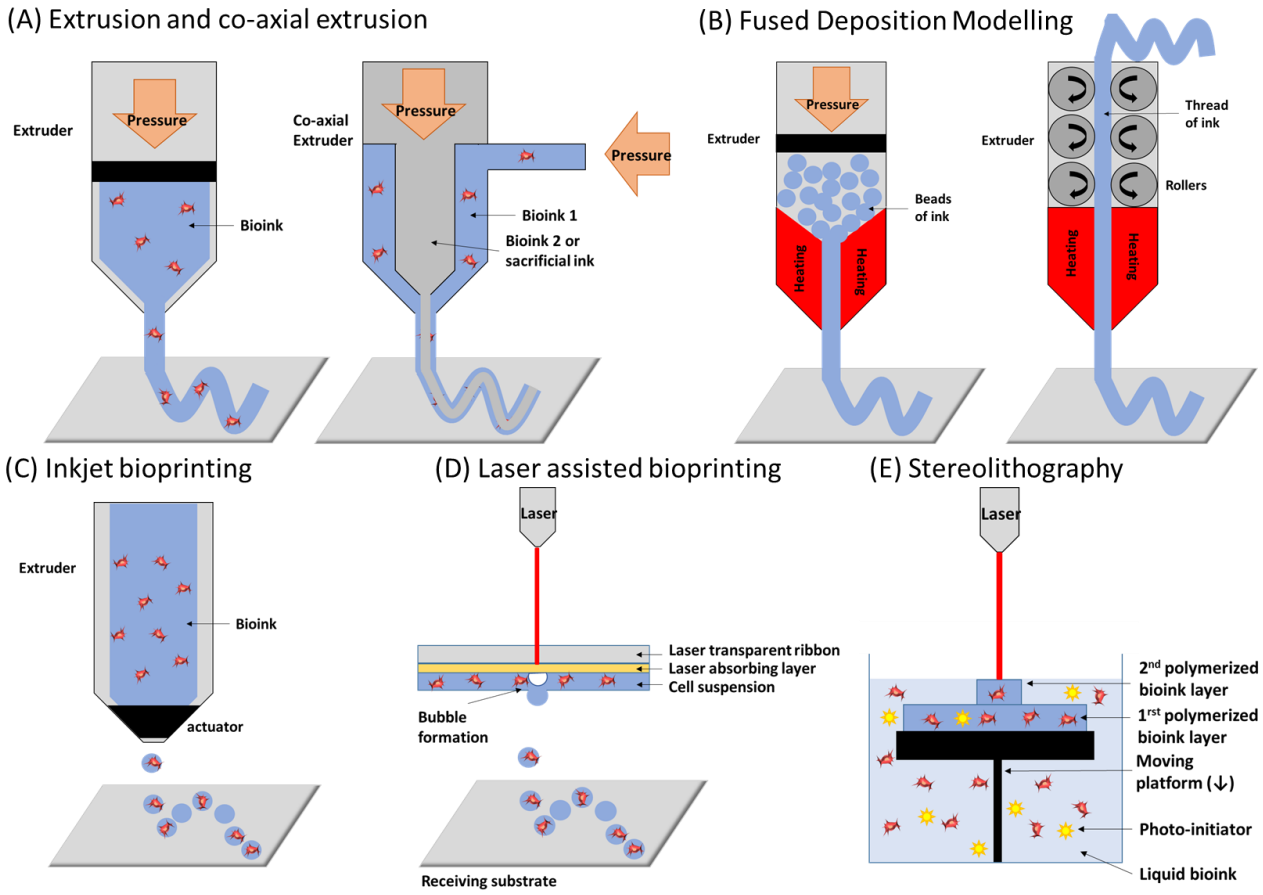

Fig. 3 Bioprinting-compatible techniques: (A) Extrusion and co-axial extrusion, (B) Fused deposition modelling, (C) Inkjet bioprinting, (D) Laser assisted bioprinting, and (E) Stereolithography.

2.2. Extrusion

Extrusion is the most commonly used technology of bioprinting. The bioink is pushed through a nozzle/tip to deliver a ribbon that will give the desired shape of a layer by x/y movement of the print head (Fig. 3A). Once the first layer printed, the nozzle moves upwards (or the receiving plate moves downwards) to print the second layer, and so on. Depending on the printer model, extrusion is induced by either an endless screw, an air compressor or a mechanical piston. Each type of device gives access to a particular range of pressure (lower for endless screw and higher for air compressor). One of the advantages of this technique is the ability to easily add extra injectors to the printer, to deliver several different bioinks in alternation or delivering the same type of ink, encapsulating (or not) different types of cells. This is particularly useful for fabricating complex multilayer and multi-area constructions. This technology is also amenable to co-axial extrusion (Fig. 3A) yielding a sheath filled with another bioink or a different ink/solution. It is particularly useful for printing, along with the bioink, either a 'sacrificial ink', which will be removed after printing, or an ink which does not contain cells but a gelator (e.g. a catalyst or a cross-linker reagent), which migrates to another bioink to induce gelation. This technique is of huge interest for vessel fabrication, and is explored in sections 4.1.2. and 4.2.2. of this review.

In contrast to other printer technologies, a bioink suitable for extrusion-based printing should have a high viscosity (from 30 to $6*10^7$ mPa/s, depending of the extruder of the printer),[22] a good shape retention once printed to avoid flooding, and a fast gelation. To increase viscosity until a 'printability' level is reached or to trigger the gelation of the bioink, extrusion can be coupled with heating or UV irradiation. Heating/cooling can be performed on the whole

extruder or just limited to the nozzle, or even on the receiving plate using the Peltier effect, as far the temperature is tolerated by cells. When required, UV-irradiation is performed either at the exit of the extruder to photo-polymerize the bioink, or directly on the printed scaffold. In the latter case, the structure should be tough enough to keep its shape until cross-linking. The flexibility of this technique means that a wide range of bioink types (i.e. chemical hydrogels and physical hydrogels) can be accommodated on extrusion-based printers. Additionally, this methodology is particularly useful for rapid prototyping and the fabrication of relatively large objects (from vessels to organ sizes). Interestingly, there is no cell concentration limitation, in comparison with inkjet, which allows only a low cell density, and laser-based bioprinting (moderate density, see Table 1). On the other hand, the high speed of material delivery is detrimental to the resolution (> 100µm).[35] Depending on the size of the cells, laboratories generally work with nozzle diameters higher than 32 Ga (0.1mm).[36,37]

2.3. Fused deposition modelling (FDM)

Fused deposition modelling (FDM) technology is quite similar to extrusion printing, but additional heating changes the physical state of the material on its way through the printer head. It is based on the fusion of a material, usually either thread-shaped or formulated as beads in the reservoir. The deposition of the melted material is then performed by a print head (Fig. 3B). This technology is widely used for thermo-responsive polymers and plastics. However its application in bioprinting remains highly limited, because of the high temperatures required for fusing the material and its plastic nature (no aqueous medium for cells), which is usually incompatible with cells. Only a few materials with either a low melting point [e.g. 60 °C for polycaprolactone and 31 °C for poly(lactide-co-caprolactone)] or a low glass transition temperature (from a rubbery and amorphous state to a glassy/crystalline state, e.g. 60 °C for polylactic acid, 16 °C for poly(lactide-co-caprolactone) and 40-60 °C for poly(lactic-co-glycolic acid)) can be used. For these reasons, this technology is often used to print non-cellularized scaffolds that will support a bioink, which is not strong enough, for example in the field of bone constructs (Table 1). Examples will be explored further in section 4.

2.4. Inkjet printing

Inkjet printing is a droplet-based method, relying on ejection of a small volume of bioink (around 20 µl) via a thermal, piezoelectric, electrostatic or electro-hydrodynamic actuator (Fig. 3C). All these types of actuators yield droplets thanks to the surface tension properties of the bioink. It is possible to print cells in culture medium, as this technique allows the handling of low viscosity inks (3-12 mPa/s).[38] By contrast, highly viscous bioinks cannot be printed. On reaching the receiving substrate, the bioink must undergo fast gelation to avoid spreading. Inkjet printers afford a very good resolution (20-100µm)[35] and proceed fast (1–10,000 droplets/s)[22] using low bioink quantities. This rapidity is reached at a lower cell viability cost than other technologies, because of the relatively traumatic expulsion of cells. In addition, this technique remains limited to the realization of relatively thin 2D objects like skin substitutes and coatings, even when they can be composed of several different printed bioink layers (Table 1).[38,39]

2.5. Laser-assisted printing

The term ‘laser-assisted printing’ comprises several techniques such as laser-induced forward transfer (LIFT),[40–42] laser-guided direct writing (LGDW),[43,44] femtosecond-laser based printing,[45] and selective laser sintering (SLS). However, only LIFT will be described here because to date it is the only laser-assisted technology that has been used to 3D print cells embedded in a hydrogel. LIFT printers are quite expensive devices. The technology relies on a laser beam that will go through a laser-transparent slide coated with a laser absorbing layer (gold or titanium) and a cell suspension, to eject droplets of the cell suspension toward a receiving substrate (Fig. 3D). To be printed with laser technologies, a bioink needs to adhere to the absorbing layer, with a low surface tension (80 mN/m seems to be the upper limit used for instance), and a low viscosity (1-300 mPa/s).[22] This technique allows a high resolution (40-300µm)[41] with a high cell viability, but with moderate speed (<10 droplets/s) compared to inkjet printing.[41] It is also devoted to 2D printing of thin layers and is very often used to print cells alone in buffer (Table 1).[43]

LIFT, like ink-jet printing, is not compatible with heating and cooling during droplet ejection, but may be equipped with a Peltier receiving plate when heating/cooling is required. Interestingly, it can be used for direct bioprinting on the body surface (animal or human).[46]

2.6. Stereolithography apparatus (SLA)

SLA uses a laser or a UV/visible light source to cross-link a bioink on the surface of a vat filled with uncured liquid bioink (i.e. an aqueous suspension of polymer and photo-initiator) containing the cells. A platform supports the first layer of printed material and goes down to allow a new layer to be photo cross-linked (Fig. 3E). The resolution is high (< 100 µm)[4] and the process is fast (< 1h for a few cm scaffold). Despite the low cost of the printer, this approach can be expensive, as it requires a large amount of bioink solution in the vat. The presence of a non-toxic photo-initiator is required and the bioink should display suitable viscosity and density to avoid cell decantation during the printing process. Conversely, there is no upper limitation to the viscosity (Table 1).[47] An alternative to SLA is digital light processing (DLP). While SLA photo polymerization is performed using a laser beam in movement, DLP is done by an image flashed with a projector. It allows faster printing of layers but requires a different apparatus.

Table 1 Comparison of the different 3D printing techniques.[48–51]

	Extrusion	Fused Deposition Modelling	Inkjet	Laser-assisted	Stereolithography
Ink viscosity (mPa/s)	< $6*10^7$	melting	3-12	1-300	No limitation
Ink requirements	Shear-thinning, shape retention	Low melting temperature	Rapid gelation	Low surface tension	Viscosity improved to reduce cell decantation, photo cross-linking
Cell density	No limitation	No limitation	Low (<10^6cells/mL)	Medium (< 10^8cells/mL)	No limitation
Amount of bioink needed	Medium	Medium	Low	Low	High
Processing speed	Fast (< 15 cm/s)	Fast (< 20 cm/s)	Fast (< 10,000 droplets/s)	Medium (< 10 droplets/s)	Fast (< 1h)
Resolution	Moderate (> 100 µm)	Moderate (> 100 µm)	High (20-100 µm)	High to medium (50-300 µm)	High (< 100 µm)
Printer cost	Medium	Low	Medium	High	Low
Current application	Shaping of 10 cm scale scaffold	Shaping of 10 cm scale scaffold	Shaping of cm scale scaffold	Shaping of mm scale scaffold; printing of cells alone	Shaping of 10 cm scale scaffold

3. Nature of bioink components

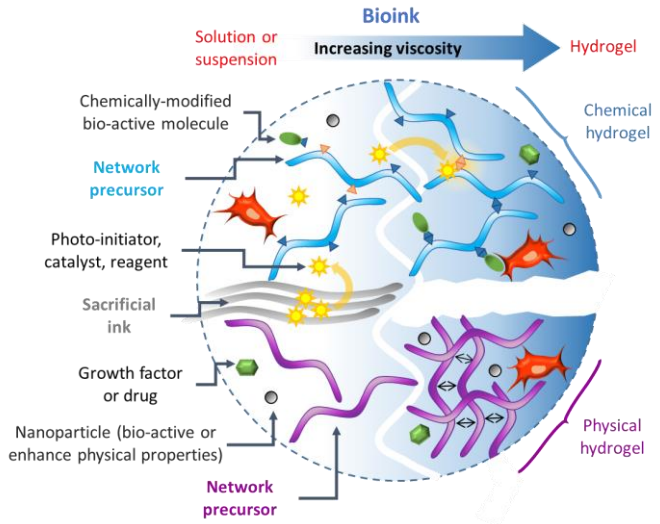

Fig. 4 Bioink composition possibilities before and after gelation.

Because of the variety of printing technologies and applications, there is no generic bioink recipe. The only common feature is that bioinks are multicomponent aqueous mixtures (Fig. 4) that contain cells. After gelation, they can produce *physical* hydrogels or *chemical* hydrogels. The cohesion of physical hydrogels is maintained by reversible interactions such as hydrogen bonds, ionic and Van der Waals interactions, while covalent bonds (usually irreversible) lock the 3D network of chemical hydrogels. Surprisingly, the number of compounds used to make bioinks is quite limited, most of the studies being based on new applications of well-known bioinks, and using combinations of these components. Studies presenting new compounds as bioink components remain quite rare. One explanation is that it takes a long time to demonstrate without any doubt good biocompatibility of a new biomaterial, and to obtain a widespread agreement among the scientific community involved in biofabrication. Bioink composition must be carefully chosen, depending on the desired properties of the target scaffold and also on the printer used (Fig. 2). This section recapitulates all hydrogel components that have been used to date for 3D bioprinting, classified according to their origin. The gelation process and applications will be treated in the section 4.

Network precursor

Besides 2D printing of cell layers that can be performed in buffers, bioinks include at least one network precursor, normally a functionalised polymer. This is the main ingredient, which provides consistency to the material and gives it its biological and mechanical properties (cell adhesion, proliferation, differentiation, robustness, flexibility, degradation, etc.). Two categories of network precursors can be distinguished: natural biomacromolecules, extracted from natural sources (plants, bacteria, genetically engineered cells, animals, etc.), and synthetic polymers. The latter mainly come from the chemical industry (e.g. Pluronic, polyethylene glycol, polycaprolactone). Natural polymers are extremely interesting bioink components as they display a superior biocompatibility compared to synthetic polymers. The main groups are polysaccharides (e.g. alginate, chitosan, agarose) and proteins (e.g. collagen, fibrin). They can be used unmodified or chemically modified to tune their properties or to facilitate their further cross-linking (e.g. methacrylated gelatin, thiolated hyaluronic acid). The modification of natural molecules usually results in improving the physical properties of the final material like higher and stronger reticulation resulting in a slower degradation and higher robustness. However, natural polymers present some drawbacks. First, they lack the reproducibility of synthetic polymers and are often more difficult to functionalize than their synthetic counterparts. Moreover, some natural materials extracted from animals, successfully used in 3D bioprinting, will never cross the barrier of clinical trials precisely because they raise safety concerns. This is the case of Matrigel™, a complex extracellular matrix produced by murine cancerous cell lines (see part 3.1.).

Doping agents, additives and delivery systems

Components that do not contribute to scaffold integrity but affording additional properties can be used. To induce cell differentiation, growth factors can also be added to the bioink, simply mixed[52–56] or chemically linked to the network.[57–59] Doping agents such as nanoparticles (e.g. hydroxyapatite[60–64]) give robustness and can also improve cell differentiation into osteoblasts. Finally, micro carriers can be added for drug and growth factor delivery.[65] They will be discussed in section 3.3.

Complex structures

Composite constructs can also be prepared by combining a bioink with a polymeric scaffold. The latter serves to support the bioink, improving the toughness of the construction. Heterogeneous layer-by-layer printing is a way of achieving the desired properties as for making cell co-cultures. These structures will be explored in section 3.3.

3.1. Natural compounds as network precursors

Many natural high-weight biomacromolecules can be used as bioink network precursors. The most popular proteins are collagen, fibrin, gelatin and silk. In the polysaccharide family, alginate, gellan gum, agarose and hyaluronic acid are used for bioprinting with variable occurrences. Finally, decellularized extracellular matrix extracts) such as Matrigel™ and self-prepared extracts are also used.

Collagen refers to a family of fibrillary proteins whose structure is organised in triple helices of polyproline-II (PP-II) type. Its primary structure is mainly composed of repeated tripeptide motives (Gly-X-Y), with X and Y being mainly proline, hydroxyproline, lysine, hydroxylysine and alanine. Its molecular weight ranges from 100 to 300 kDa. Collagen is the major protein component of the extracellular matrix (ECM). Collagen type I is by far the most used for biomedical applications and bioprinting because it represents 90% of the collagen present in the human body, mainly in skin, bones, tendons and organs. It is extracted from animals, usually rat tail, or can be produced by recombinant bacteria. With its highly hierarchized and organized structure, extracted collagen must be treated to yield liquid homogeneous solutions suitable as bioinks. This is achieved by enzymatic or acidic treatment. The latter is often preferred over enzymatic treatment because pepsin cleaves amino acids from the C and N terminal regions of tropocollagen, which normally contribute to trigger re-assembly in fibrils. Collagen presents no cytotoxicity, good cell adhesion, can be biodegraded by collagenase, is easy to prepare, and can make a hydrogel at low concentration (from 1.5 mg/ml).[48,50,66]

Gelatin is a derivative of collagen, extensively used in the food industry, and a common network component of bioinks. Gelatin is obtained by prolonged boiling of bones and conjunctive animal tissues (bovine and porcine origin), which denatures the collagen organisation resulting in defibrillation and loss of the triple helix structure (Fig. 9). Its molecular weight goes from 100 kDa to 20 kDa depending on the product used. Once solubilised in water, gelatin gives a physical hydrogel once cooled to room temperature. It presents no cytotoxicity, good cell adhesion, faster biodegradability than collagen, is easy to prepare, and is very cheap, thus being a good candidate for bioprinting. Its properties can be improved once chemically modified (see 3.3.).[48,50] However, since the protein is shorter and much less organized than collagen, it needs a higher concentration to gelate (from 10 mg/ml).[66]

Fibrin is a fibrous protein obtained by thrombin-catalysed polymerization of fibrinogen (~340 kDa) during blood clotting.[67] It has good cell adhesion, it is biodegradable, and is not very stable in the long term. Fibrin may induce an inflammatory response in some cases, or a thrombus. Pairing of fibrinogen and thrombin is particularly useful as a two component bioink which may gelate once in contact (see 4.2.3.1.).[48,50]

Silk is a protein-based biomaterial produced by worms (commercially), which can be use as a bioink precursor. Silk is formed by fibroin proteins (100-450 kDa) with inter and intra strand beta sheet structures (Fig. 5E). To be used as a bioink, silk needs a treatment before gelation consisting in breaking H-bonds between sheets to be solubilized. Silk-based bioinks present good cell adhesion and degradability.[68]

Alginate is the most used biopolymer for bioprinting. This polysaccharide (Fig. 5A) is extracted from brown algae. It is composed of β-D-mannuronate (1.4)-linked to C-5 epimer α-L-guluronate, with a molecular weight varying from 10 to 200 kDa. It is biodegradable, biocompatible and induces no inflammatory response but presents a relatively modest cell adhesion compared to other biopolymers.[69] Its most attractive feature lies in the very simple way gelation is triggered, by the addition of a non-toxic divalent cation (e.g. Ca^{2+}). It can reach different viscosities depending on concentration, allowing alginate to be printed with various instruments.[48,50]

Gellan gum is an anionic polysaccharide (Fig. 5B), very close to alginate in terms of implementation (cation-triggered gelation) and physico-chemical properties. It is a tetrasaccharide consisting of two D-glucose units, one of L-rhamnose and one of D-glucuronic acid, with an average molecular weight of 500 kDa. This polysaccharide is extracted from the *Sphingomonas elodea* bacteria and gives a transparent hydrogel. Like alginate, gellan gum presents very poor cell adhesion compared to other natural polysaccharides used as bioinks.[48,50,69–71]

Hyaluronic acid (HA), also known as hyaluronan, is a glycosaminoglycan extracted from bacteria (genetically modified *Bacillus subtilis*) (Fig. 5C). It is constituted of an unbranched disaccharide repetition unit composed of D-glucuronic acid and D-N-acetylglucosamine. Several HA formulations have been approved by the FDA. HA is a major component of the human extracellular matrix, giving elasticity and hydrophilicity to tissues, and therefore displays very good cell adhesion, biocompatibility and biodegradability by hyaluronidase.[72,73] Nevertheless, to obtain a HA-based hydrogel, it must be used at high concentration (> 2 mg/ml) or to be chemically modified.[48,50] In the body, it can have a molecular weight varying from 10 to 10000 kDa depending on its origin, and it is commercially available in many sizes.

Cellulose is a biopolymer made up of D-glucose units. It comes from plants and wood. Cellulose by itself does not yield hydrogels. However, methylcellulose (Fig. 5D), nanocellulose (nano-sized cellulose fibers) and other cellulose derivatives are suitable for hydrogel's formation. They are obtained by chemical modifications of cellulose. Although cellulose is biocompatible, it presents low cell attachment properties and is non-degradable by human cells.[74] It is mainly used as a supporting material for other bioinks.[48,50,74]

Agarose, a seaweed-extracted polysaccharide, with D-galactose and 3,6-anhydro-L-galactopyranose repetition units, (~120 kDa, Fig. 5F) is commonly used in molecular biology to make hydrogels. Agarose is easy to print but unfortunately suffers from a low cell attachment although it is biocompatible and can be degraded by cells.[75]

Decellularized containing extracellular matrix (dECM) can be used as bioink. These complex protein mixtures can be obtained from any cell culture in laboratory, using specific protocols (extraction from native skin,[76], heart tissues,[52] adipose tissue and cartilage).[52,77,78] dECMs include structural proteins like collagen, laminin and nidogen, but also growth factors and small quantities of other proteins. Thanks to its inherent properties, ECM components and growth factor cocktails are highly favourable for cell proliferation and differentiation, and to its viscosity, from 10^6 mPa/s in non-diluted state and lower after dilution, they are very attractive bioactive and easy-to-print bioinks. However, dECMs are physical hydrogels presenting low elasticity and stiffness.[48,50] Among dECMs, Matrigel™ is a commercially available bioink. It is produced by a mouse sarcoma cell line (Engelbreth-Holm-Swarm, EHS) and marketed as support for cell culture. The complex composition of Matrigel™ is one of its major advantage as it recapitulates the features of natural ECMs.[79,80] The downside of dECM, including Matrigel, is that these materials are not quantitatively and even qualitatively defined and display significant variability between batches. Despite its popularity and efficiency for cell culture,

Matrigel™ remains a support for bioassays, and it is very unlikely that such a material could one day be injected in humans, for safety and ethical reasons (i.e. infection, immunogenicity).[48,50]

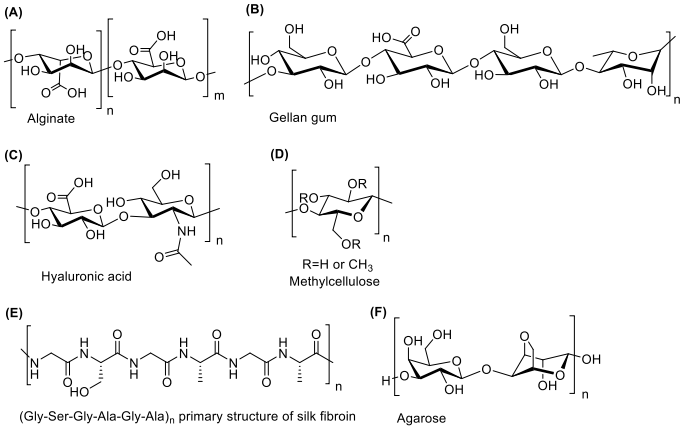

Fig. 5 Biopolymers used as bioink components: (A) alginate, (B) gellan gum, (C) hyaluronic acid, (D) methylcellulose, (E) silk fibroin, and (F) agarose.

As mentioned before, biomacromolecules can also be chemically modified, keeping their inherent, interesting properties, and adding new ones. Some do not gelate and cannot be used as a bioink. They must be reticulated to form a hydrogel network. Chemical modifications can also afford additional properties (e.g. speedy gelation, slow degradation, possibility of backbone grafting of other active molecule-modifying rheological properties). Chemical modifications of biopolymers will be presented in section 4.2.1.

3.2. Synthetic compounds as network precursors

Mostly bio inert and displaying poor cell viability compared to natural biopolymers, synthetic polymer-based bioinks must be supplemented by other components. They may also serve as supports and intercalated layers in composite materials, to improve the mechanical properties of the final constructs.

Poly(ethylene glycol) (PEG, Fig. 6A and 6B) is FDA approved and displays good biocompatibility. However, it is poorly adherent to cells and lacks biodegradability.[50,81] It is commercially available in several shapes, in linear or branched geometries (3, 4, or 8 arms), and in various sizes from 0.5 to 20 kDa. To be used as a hydrogel, it needs to be cross-linked (see 3.3.).

Polycaprolactone, polylactic acid and copolymers of them[82] (PCL, PLA, poly(lactide-co-caprolactone, PLCL Fig. 6C, D and E respectively), like polyesters, cannot be used to encapsulate cells, as they are water insoluble plastics.[50] However, they are biocompatible and they represent interesting choices as cell-free supporting materials. The ester linkage can be degraded slowly by lipase and esterases. The reported degradation time of PLA ranges from 10 months to 4 years, depending on the size[83] and of the porosity. It may be even longer for PLCL, yielding hydroxyhexanoic acid and lactic acid. Thus, a bioink used in alternation with these polyesters will likely be degraded long before it, increasing the scaffold's stiffness during the life of the hydrogel. PCL and PLA have been approved by the FDA for the preparation of medical devices (e.g. implants for drug delivery, screws and plates).[84] They are stiff, biocompatible and cheap materials that can be extruded by FDM at their glass transition temperature is of 60 °C for PCL[50,85,86] and of 65°C for PLA.[87,88]

Pluronic F127 (x = 110 and y = 70, 12.5 kDa, Fig. 6F) is a poloxamer, which is principally used as a sacrificial ink when suspended in an aqueous solution. It undergoes a temperature-dependent sol-gel transition, being liquid below 10 °C, and gelifying at a higher temperature. At low temperature, pluronic is present as a unimer state. It forms micelles by desolvation of hydrophobic chains, which interact with each other to yield the hydrogel network when the temperature rises up. Its good water solubility and thermos-responsiveness make pluronic particularly attractive to use as a sacrificial ink. [50,89,90] Indeed, once shaped at low temperature, pluronic printed areas can be easily removed by water washings.[50,89,90] This is particularly useful when long gelation times of other bioinks are required, as it serves as a temporary supporting matrix. It may be used to create holes in the final material for vessel printing. Another smart use of pluronic is to reduce the toxicity of some compounds (catalysers or cross-linkers) which are required for bioink gelation by adding it inside the pluronic layer instead of the

bioink.[64,65,91] Compounds migrate slowly from the pluronic to the bioink, being present at lower concentration and over a longer period of time than if they were simply mixed with the bioink, thus reducing the toxicity and improving cell survival.(Fig. 7D).

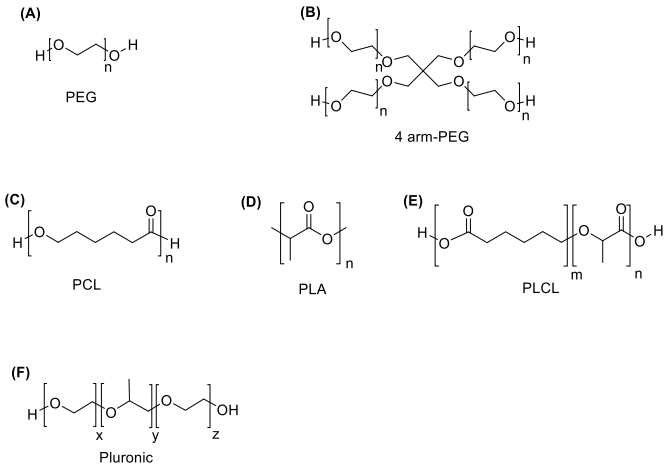

Fig. 6 Synthetic polymers commonly used as inks: (A) polyethylene glycol; (B) 4 arm-PEG; (C) polycaprolactone; (D) polylactic acid; (E) polylactide co-caprolactone; and (F) Pluronic F127.

3.3. Composite and complex constructs

As just discussed, printed scaffolds may sometimes be advantageously composed of two or more different inks, where at least one is a bioink. These complex constructions could be classified in three categories:

- Composite structures with alternating bioink and plastic (i.e. dry polymeric material) layers, the latter being merely a rigid backbone structuring the scaffold;
- Heterogeneous structures obtained by printing different bioinks/ink layers of different compositions;
- Complex structures in which various objects are included in the bioink. These may be nano-carriers for drug delivery, nanoparticles or chemicals.

It is worth noting here that we do not consider 'complex constructs' scaffolds obtained by alternating layers containing or excluding gelation catalysts (e.g. photo initiators, $CaCl_2$).

Composite structures

The rigid part of these scaffolds is always made from PCL and PLA printed by FDM or regular extrusion, heating at glass transition or melting temperature. This structure can be used as a mold circling the hydrogel to prevent flooding, or as tougher layers in between bioink layers (Fig. 7A, B and C). This procedure is extensively used to produce bone and cartilage grafts where PCL or PLA layers are combined with alginate, agarose, gelatin or Matrigel™ bioinks,[53,54,60,92–96] and has also proved to be useful as a robust cell culture platform.[97] The plastic and the bioink are usually extruded with a multi-head printer.

Heterogeneous structures

The most common heterogeneous structures are obtained by printing successive superimposed layers (2 or 3), each composed of a different bioink. Each bioink can contain specific cells, but may also include different network precursors. For example, a cross-linker or a reticulation agent (cation, enzyme, photo-initiator, etc.) can be included in a different ink (typically Pluronic) than the one containing the network precursor. However it can also be used in two-step cross-linking, for example fast physical gelation followed by chemical cross-linking, to change the physical characteristics of the hydrogel (degradation, rheology, etc.). As already stated, one of the inks can be a temporary template removed after printing (Fig. 7 D and E). The removal of the sacrificial ink must be as simple as possible without inducing the structure collapse. Tubes have been printed by coaxial extrusion of Pluronic (inside) and a mixture of alginate and dECM embedding cells (outside) to generate blood vessels.[65] Alternatively, sacrificial ink has also been used to support gelatin methacrylate-encapsulating cells during the proliferation and differentiation of the co-culture. Pluronic, which supported the bioink deposition, was removed once the cells had created their own ECM, yielding a biomaterial stiff enough to keep its structural integrity.[10]

Both the two strategies, cell co-culture using two different bioinks, and the use of sacrificial ink to make

hollow structures, have been combined to create vascularized tissue constructs.[98]

Complex structures

This category includes two groups of compounds, nanomaterials and chemicals that display various new properties.

Complex constructs can be obtained by doping an ink or a bioink with nano objects. This is mainly used to improve the physical and biological properties of the hydrogel. Gold nanorods were added to give electrical properties and to improve cell signalling between cardiac cells.[99] Introduction of micro-carriers gives higher compressive strength[100] and allows delivery of drugs and growth factors.[65] Organic and inorganic nanoparticles are used to improve cell differentiation (e.g. hydroxyapatite[60–64]). and stiffness.[101,102] Spheroids, i.e. small spheres of hydrogel containing cells inside, can also be added to have a different cell distribution inside the scaffold.[103]

Addition of chemicals into bioinks can tune their properties. Hydrogel physical properties can be modified by adding polyvinylpyrrolidone (PVP), a macromolecule giving a "high fractional volume occupancy" (FVO) to enhance the excluded volume effect. This results in high volume pores into the hydrogel, thanks to its high size.[104] Studies have demonstrated that the addition of PVP into bioinks improved its homogeneity, as well as the viability of printed cells during and after bioprinting.

On the other hand, the hydrogel can be covalently modified by bioactive molecules. It can be modified with substrates of matrix metalloproteases (MMP), which are used as spacers by linking two different polymeric network precursors. Upon MMPs release by cells from the culture, the peptide sequence is cleaved, specifically releasing the network and decreasing the degradation time.[57,58] It is also possible to add drugs,[60,65] peptide ligands improving cell adhesion like the integrin ligand RGD[57–60,105,106] and differentiation factors.[54] In these cases, the bioink itself acts as a reservoir for drug/bioactive compound delivery. The design of hydrogels to deliver fragile bioactive ingredients such as therapeutic proteins or peptides, in a time and spatially resolved manner is a very important field of research, and the subject of comprehensive recent reviews.[107–112] Studies carried out in this area will undoubtedly cross-fertilize the field of biofabrication.

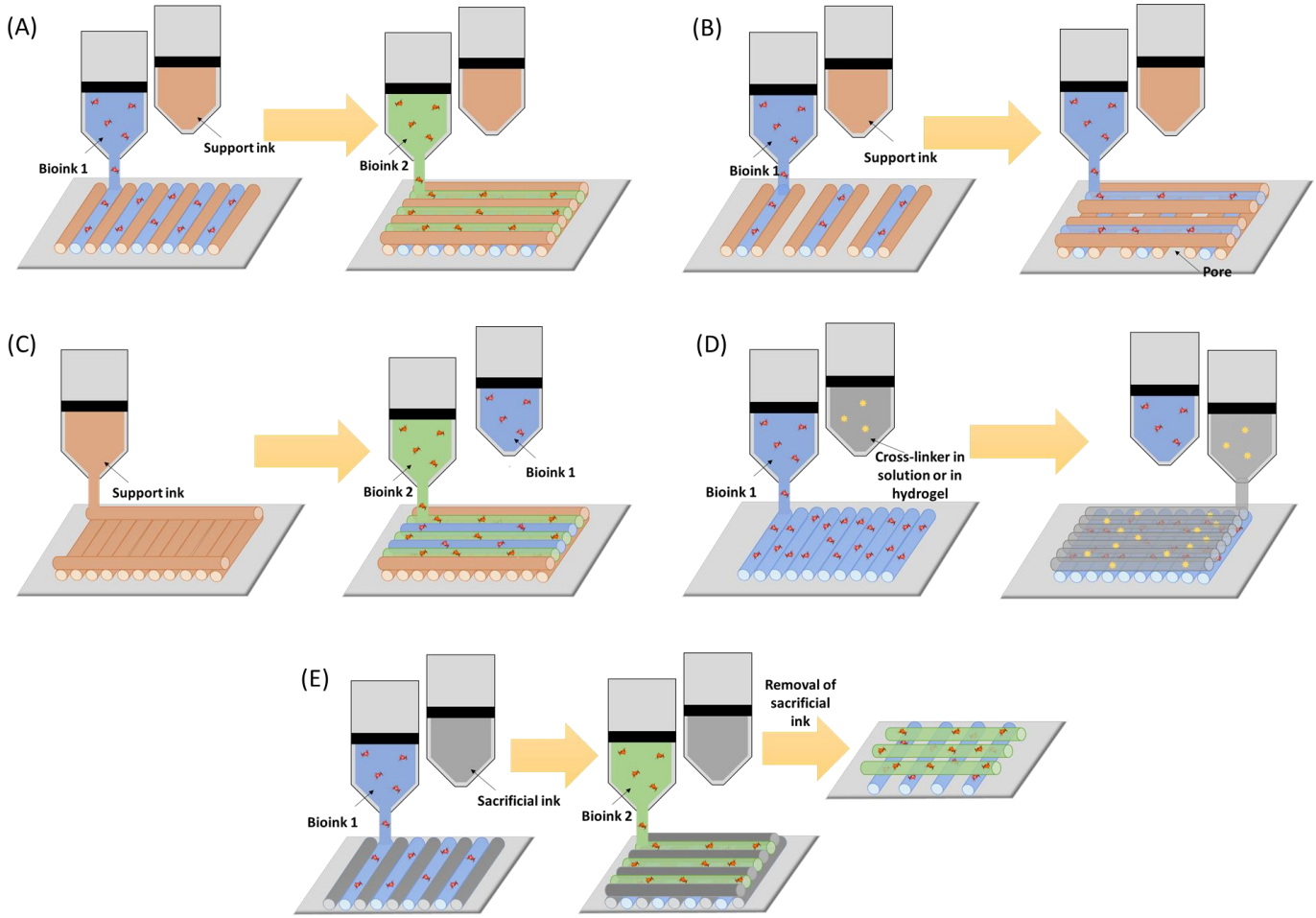

Fig. 7 Printing of composite scaffolds containing a plastic support ink (A[54,96,113,114], B[5,53,60,77], and C[52,95]), and examples of heterogeneous scaffolds containing at least two non-plastic (bio)inks (D[115–117] and E[10,91]).

4. Physico-chemistry of gelation

Depending on the nature of the network precursors, a bioink can turn into a physical or a chemical hydrogel. As explained earlier, the integrity of a physical network is stabilised by weak interactions. In the case of a chemical hydrogel, the gelation occurs upon establishment of covalent bonds formed between reactive groups present in the network precursors (e.g. polymers) and/or additional bi- or multi-functional cross-linkers. In all cases, physicochemical parameters such as temperature and concentration of precursors have an impact on the gelation kinetics, on the final appearance and properties of the printed hydrogel scaffold. The following parts of this review describe the different gelation physical or chemical processes and the main classes of network precursors. All the reviewed examples will also be presented in three tables (Tables 2 to 4) at the end of this review, sorted by the mechanism of gelation used.

4.1. Non-covalent assembly (i.e. bioinks based on physical hydrogels)

The physical assembly of molecules and macromolecules into a hydrogel by non-covalent bonds is generally reversible. Thanks to shear-thinning (i.e. thixotropic) properties, the hydrogel can go back to a liquid state upon compression or stirring, simplifying the 3D printing process. Physical hydrogels containing bioink are easy to prepare and numerous network precursors are commercially available, allowing gelation after solubilisation. Gelation is fast and biocompatible; it generates no side product and does not require any additional chemical reagent (e.g. photo initiator, coupling reagent) with the exception of ions in the case of

ionotropic gelation. The downside is that physical hydrogels undergo a faster degradation compared to chemical hydrogels, and present relatively weak mechanical properties. It implies that they cannot be used for long-term scaffolding. However, they present good self-healing post printing properties with no mark of extrusion, no interfacial area, etc., and low shear stress, compatible with all 3D-bioprinting technologies except stereolithography, which needs covalent UV cross-linking (see 4.2.2.).

Among the physical gelation driving forces, one can distinguish weak inter- and intra-molecular interactions such as self-assembly, aggregation and coacervate, and ionotropic gelation (Fig. 8). All examples are assembled in Tables 2 (physical gelation-based bioinks) and 4 (complex bioinks).

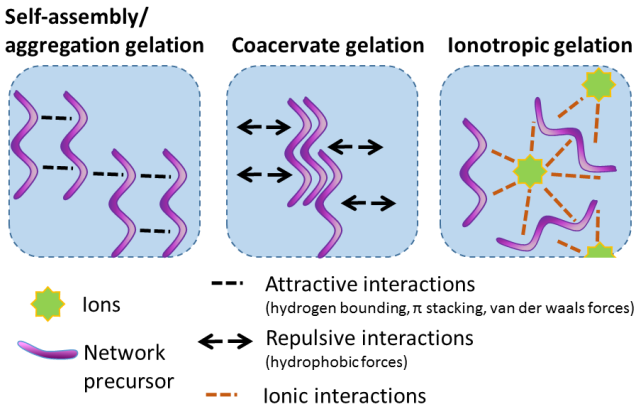

Fig. 8 Gelation process of physical hydrogels: self-assembly-driven gelation, coacervate and ionotropic gelation.

4.1.1. Weak binding forces (coacervate gelation, self-assembling, etc.)

Self-assembling of network precursors, through hydrogen-bonding, π-stacking, hydrophobic and van-der-Waals forces, can give a suspension viscous enough to yield to a printable material (Fig. 8). The nature of these forces depends on chemical formula of the network precursor (i.e. the biopolymer). When there is a specific recognition of sequences, we talk about self-assembly, whereas when it is just assembly by weak binding without specificity we talk about aggregation. Coacervate is made by combination of attractive forces between biopolymer chains, but mainly by repulsive hydrophobic interactions with the solvent, leading to gelation. Common physical bioinks are collagen, hyaluronic acid and gelatin, which can turn into a hydrogel by formation of hydrogen bond networks.

4.1.1.1. dECM-based bioinks

The poor physical properties of decellularized extracellular matrices are counterbalanced by the high cell viability observed within such materials after 3D printing. dECM suspension into PBS or culture medium (10-30 g/l) gives a viscous hydrogel principally by self-assembly. These hydrogels have been used for 3D bioprinting alone by extrusion or combined with a PCL printed framework[77] to circumvent its poor Young's modulus.

Li *et al.*[118] mixed Matrigel™ with various concentrations of hydroxypropyl chitin to extrude it with moderate heating (15-37 °C). Murphy *et al.*[113] extruded droplets of Matrigel™ bioink on the top of PCL layers containing 13-93B3 borate glass, which promote angiogenesis.

4.1.1.2. Collagen-based bioinks

Commercially available collagen can be provided as lyophilized fibrous material, or more conveniently, already solubilized in acidic solution (HCl or acetic acid, pH ≈3) at 1 to 10 mg/ml. At low pH, peptide chains are globally positively charged. The PP-II and the tropocollagen triple helical assembly are conserved, but repulsive forces arising from charge repulsion disturb the self-assembly of fibers, resulting in a homogeneous liquid solution mostly composed of isolated tropocollagen. This stock solution is then poured into neutralizing buffer (e.g. PBS with sodium hydroxide). After about 30 minutes at 37 °C, a hydrogel is obtained thanks to the re-assembly of fibrils and then fibers. This assembly is driven by hydrogen bonding between amino acids belonging to different collagen chains and steric constraints.

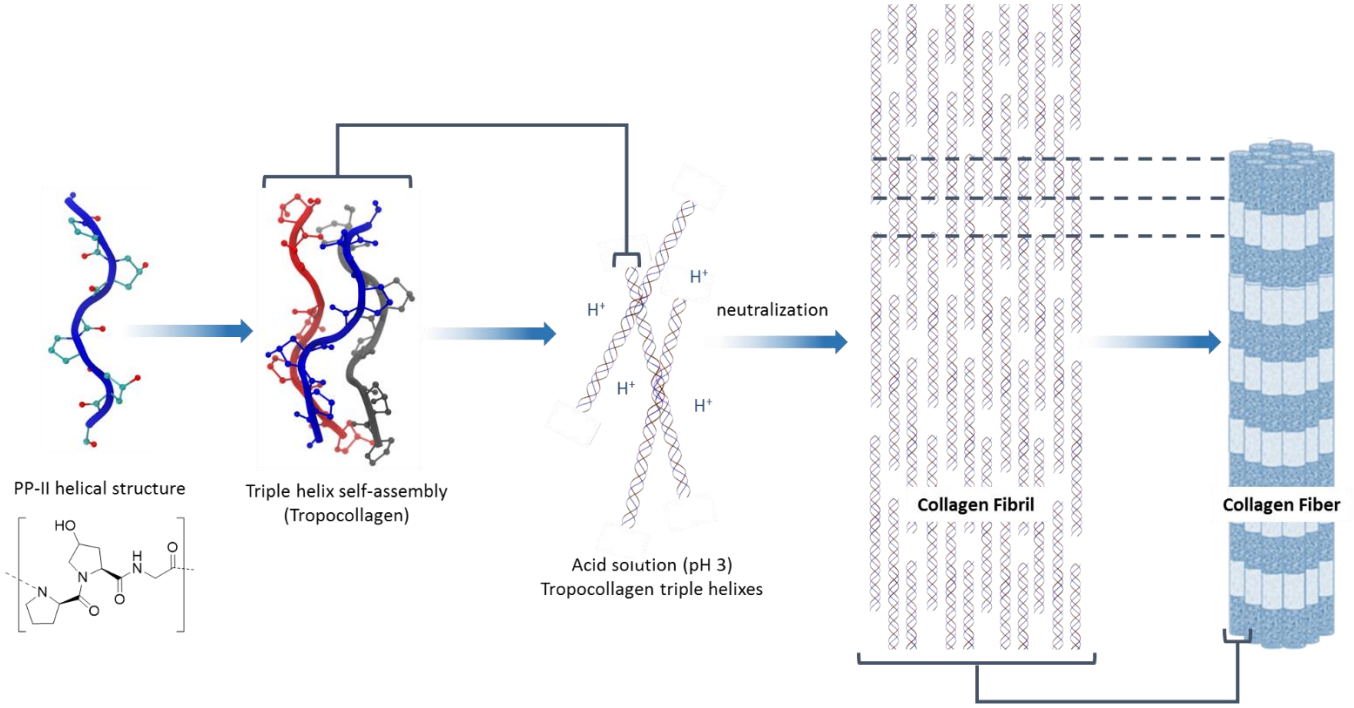

Fig. 9 Hierarchical assembly of collagen into fibrils and fibers in acidic solution upon neutralization.

At low concentrations (< 1 wt%) collagen is suitable for droplet ejection,[119] inkjet[104] and laser-assisted 3D bioprinting.[46] At higher concentrations (above 1.25 wt %), it reaches a viscosity suitable for extrusion.[120]

4.1.1.3. Hyaluronic acid-based bioinks

Thanks to intermolecular hydrogen bonding and strong interactions with water molecules, hyaluronic acid can turn into a viscoelastic hydrogel with random coil organisation and lubricant properties.[73] It can be used alone, but it is more commonly used in combination with another biomacromolecule (e.g. methylcellulose) to improve the physical properties of the bioink mixture by reducing the swelling for extrusion.

4.1.1.4. Silk-based bioinks

Silk fibroin has the ability to undergo sol-gel transition in water under stimulated conditions (shearing, solvent removal, heating, sonication, addition of salts, etc.).[121] This is due to its propensity to form intra- and inter-molecular antiparallel β-sheet structures, thanks to hydrogen bonding between C=O and NH groups of amides in the Ser-Gly-Ala structure (Fig. 10). Indeed, β-sheets are dynamic structures privileged when self-assembly is induced by increased concentration, heating or addition of other aggregation and self-assembly inducing compounds. Interestingly, the sol-gel transition can be also provoked by addition of polyethylene glycol chains. This Fibroin/PEG mixture has been used as a bioink for extrusion.[122]

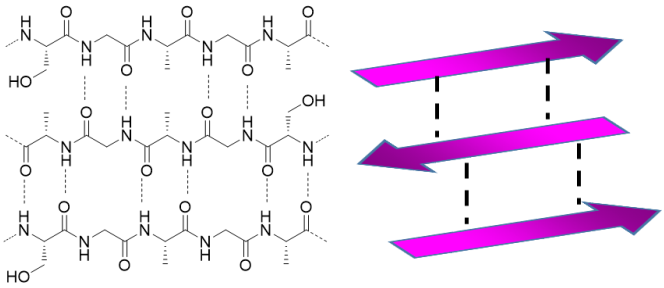

Fig. 10 Self-assembly of silk fibroin peptide sequences in antiparallel β-sheet structure.

4.1.1.5. Agarose-based bioinks

At low temperature, usually below 45°C, but it can be lower depending on the different chemical structures and molecular weights of agarose that are used, agarose solutions undergo a thermic hysteresis liquid-solid phase transition, leading to hydrogels formation thanks to intra- and inter-molecular hydrogen bonds, giving double stranded helices and water retention inside the hydrogel cavities (Fig.

11).[123] Because of its low cell attachment property, agarose is often mixed with collagen.[100] It has also been combined with short dipeptide gelators that self-assemble (e.g. Fmoc-diphenylalanine and Fmoc-isoleucine-glycine), and collagen for droplet ejection into an oil vat.[124] An emulsion is formed by organization of a lipid monolayer around the bioink droplet (Fig. 12). A mixture of agarose and collagen has also been used along cell-laden poly(D,L-lactic-co-glycolic acid) (PLGA) porous microspheres,[100] yielding a complex bioink with improved compressive resistance and cell viability suitable for extrusion.

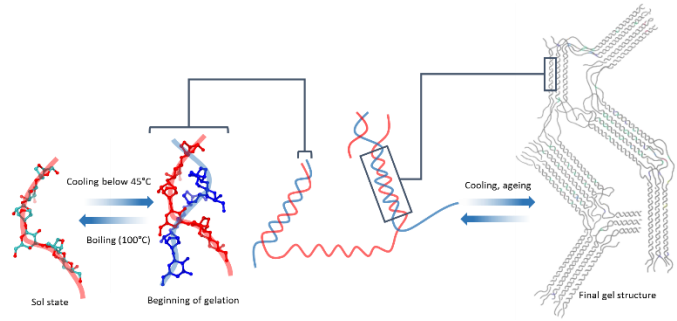

Fig. 11 Gelation process of agarose.

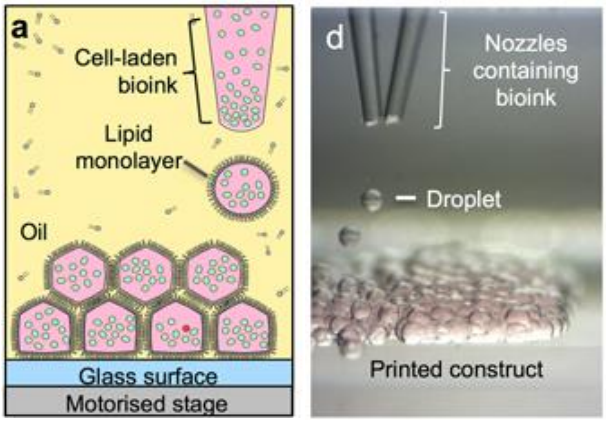

Fig. 12 3D bioprinting of bioink composed of agarose, dipeptides and collagen, into an oil vat (from ref 124).

4.1.1.6. Thermo-sensitive bioinks

Thermo-sensitive polymers have the ability to change from a sol/coil state to a gel state by aggregation (e.g. for PNIPAM compounds) or formation of micelles (e.g. for Pluronic and other poloxamers, Fig. 13) with temperature increase, upon reaching the lower critical solution temperature (LCST).[125] Indeed, when the temperature is above the LCST, the hydrophobic part of the polymer aggregates to form micelles and the hydrophilic part dehydrates, leading to aggregation of micelles, and to a viscosity increase.

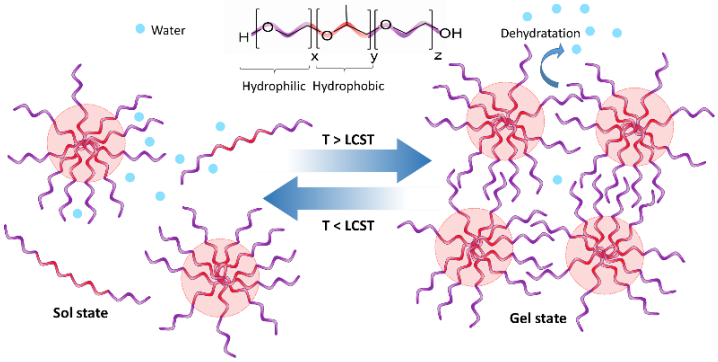

Fig. 13 Thermo-sensitive polymer structure transition.

Lorson *et al.*[126] developed block copolymers made by ring opening polymerization of hydrophilic poly(2-methyl-2-oxazoline) and thermos-responsive poly(2-n-propyl-2-oxazine) (nPrOzi) (Fig. 14) that have been used in solution. The block copolymer solution becomes a hydrogel at temperatures higher than 30 °C, which is quite useful for 3D printing cells at 37 °C by an extrusion process. Indeed, while passing through the nozzle, the bioink is liquid but turns into a gel once in contact with the heated collector surface.

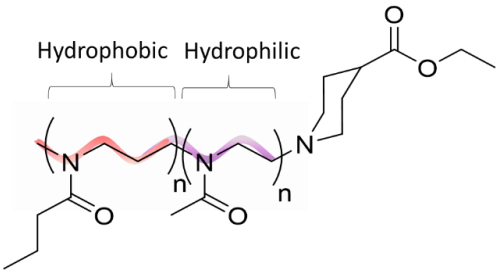

Fig. 14 Block copolymer synthesized by ring opening polymerization of poly(2-methyl-2-oxazoline) and poly(2-methyl-2-oxazine).[126]

With a similar strategy, Hsieh *et al.*[127] developed a thermos-responsive bioink (i.e. gelation above 37 °C) containing stem cells, adapted to extrusion printing. They used an aqueous suspension of nanoparticles made out of two different polyurethane (PU) derivatives, a copolymer of poly(ε-caprolactone) (PCL) diol that provides soft properties, and poly(L-lactic)acid (PLLA) diol or poly(D,L-lactic) acid (PDLLA) diol, with incorporation of isophorone on the

polymeric chain and of a urethane bond in-between (Fig. 15). These PU are biodegradable and their rheological properties can be tuned by variation of the PU derivative concentration. Moreover, the crystal structure of PLA, which is dictated by its conformation, has an influence on both cell proliferation, which is better for PDLLA-containing PU, and differentiation, which is better for PLLA-containing PU. The hydrodynamic diameter of the particles increases from 34-38 nm at 10 °C to 44-48 nm at 37°C, due to heating-induced swelling.[128] The diameter increase also allows negative charges to be pushed away from the surface of the NPs, decreasing repulsion between them, and leading to aggregation of NPs to form a hydrogel.

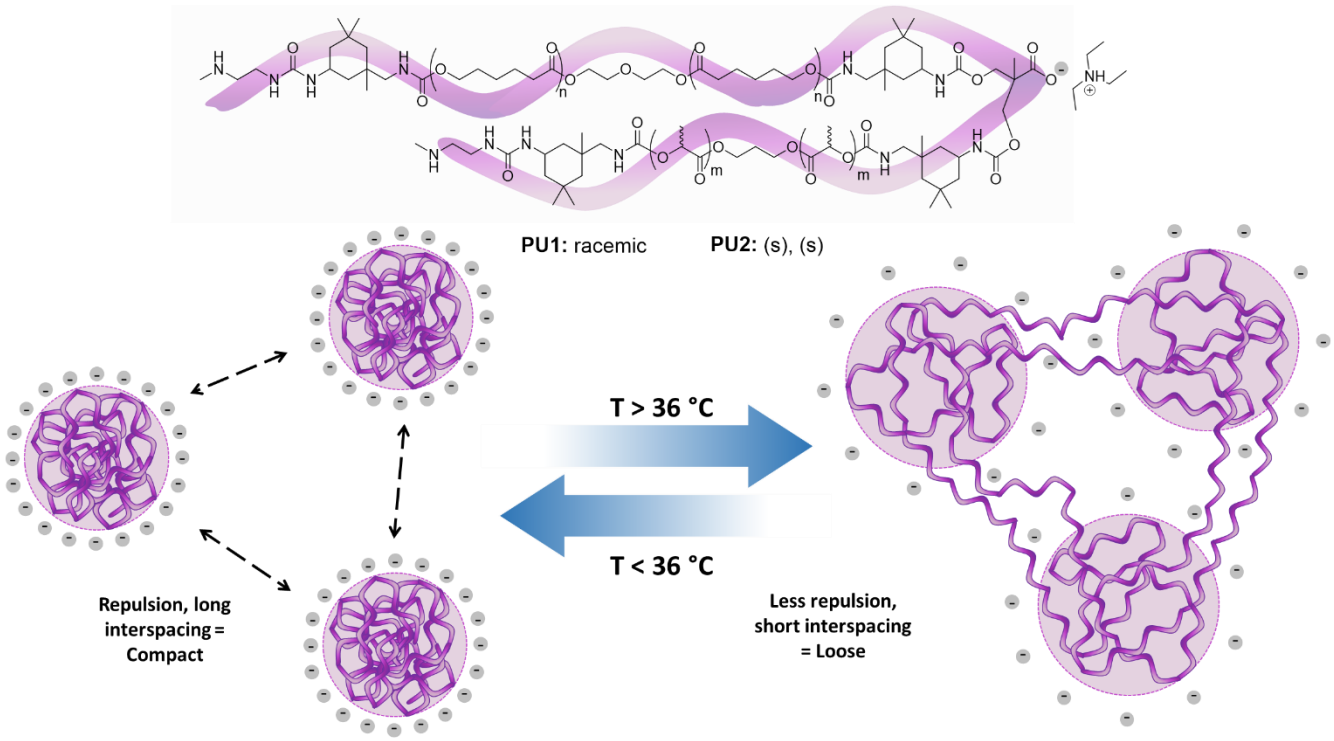

Fig. 15 Precursor of nanoparticles giving thermos-responsive bioink, nanoparticles and gelation upon heating.[127]

4.1.1.7. Peptide- and DNA-based bioinks

Thanks to the diversity of amino acid side chains, to the hydrogen bonding properties of the amide bond, and to the variety of secondary structures of peptides, many peptide sequences are able to self-assemble through non-covalent interactions such as hydrogen bonds, π/π stacking, and hydrophobic interactions, leading to the formation of supra molecular structures. β-sheet forming peptides are among the most widely studied for hydrogel formation,[129,130] especially in the field of drug delivery,[131] but some of these peptides have been recently used as bioink components. Upon reaching a sufficient concentration and depending of the peptide's structure, they form fibrils that grow in a 3D network of entangled fibers, turning the solution into a physical hydrogel. This is the case for Gly-Ala-Ile-Leu from 17 wt%, to 0.01 wt% for PTZ-Gly-Phe-Phe-Tyr.[129] Commercially available β-sheet-forming peptides were already available for extrusion bioprinting (e.g. from PeptiGelDesign).[132] On the other hand, amphipathic peptides bearing a hydrophobic N-terminus and a cationic hydrophilic C-terminus (e.g. Ac-ILVAGK-NH_2[120]) have the propensity to assemble in stable helical supra molecular structures, which induce gelation in less than 10 seconds at 37 °C in the presence of cells.

Bioinks based on short peptides are fully synthetic and do not suffer of natural biopolymer problems like batch-to-batch reproducibility. Moreover, they are easy to modify, and to add additional properties to the network. Unfortunately, they form physical hydrogels whose mechanical properties are not easily tuned, and they can be quite expensive especially when large volumes of scaffold have to be printed.

A few bioinks have been developed on the basis of oligonucleotide sequence specific recognition. For example, Li *et al.*[115] proposed a bi-component bioink made of a polyGlu–DNA conjugate and a double-stranded DNA (dsDNA). The two components are deposited alternatively by inkjet printing with high accuracy. Upon diffusion, the fast hybridization of the polyGlu-DNA conjugate and the dsDNA (Fig. 16) yields a hydrogel with good self-healing properties. It is noteworthy that this hydrogel can undergo enzymatic degradation by peptidases and nucleases.

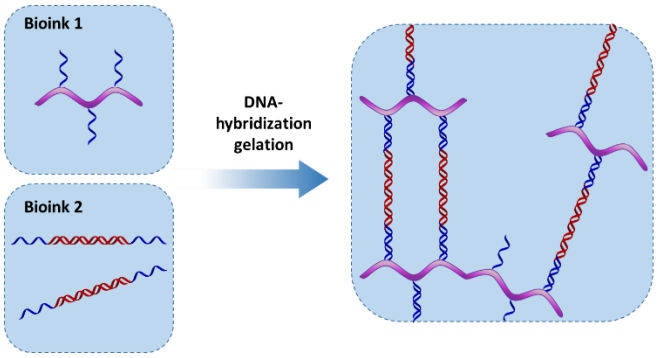

Fig. 16 3D bioprinting of a two components bioink using DNA hybridization strategy. Poly(L-glutamic acid240-co-g-propargyl-L-glutamate20) in purple, single strand DNA conjugate in blue, double stranded DNA in red.[115]

The property of guanosine to form tetrameric assemblies in water, in the presence of monovalent cation such as potassium or sodium (i.e. G_4-quartet structure), was exploited by Biswas *et al.*[133] to develop a bioink. Indeed, tetramers stack on the top of each other to from nano-fibers, which entangle in a 3D network. This hydrogel is highly thixotropic and has self-healing properties allowing its easy extrusion providing good cell viability.

4.1.1.8. Host-guest interaction-driving gelation

Host-guest chemistry is driven by self-recognition and non-covalent interactions between two chemical entities (e.g. a receptor and a ligand) forming an extremely strong and stable complex. An example of host-guest interaction is the assembly of cucurbituril, a macrocycle made of glycoluril units bound together by methylene bridges, with alkyl chains inside its hydrophobic cavity.[134] K. Kim's and D.-W. Cho's teams[54,135] have used this tandem to develop a complex construct using four different inks. The first ink is PCL, printed as a supporting scaffold for the overall construct made of two bioinks containing cells and two different growth factors, and another ink. One bioink is composed of collagen, and the other contains functionalized hyaluronic acid with the host [Cucurbit[6]uril-hyaluronic acid, (CB[6]-HA)]. Finally they extruded the forth ink, which contain hyaluronic acid functionalized with the guest: 1,6-diaminohexane-hyaluronic acid (DAH-HA). The CB[6]-HA and the DAH-HA (Fig. 17) assembled together by a host-guest mechanism. The weak interactions between hyaluronic acid chains improve the viscosity of the construct.

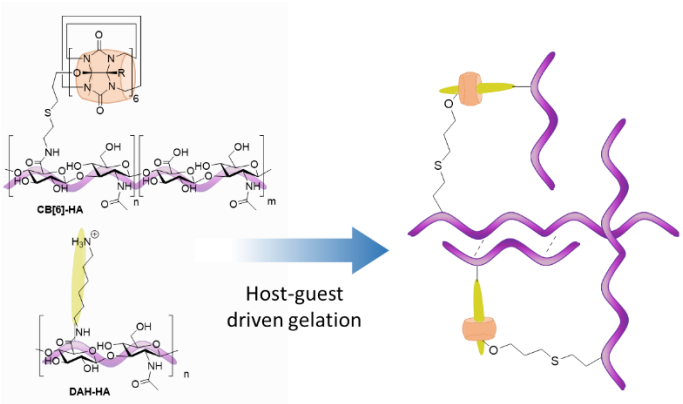

Fig. 17 Host-guest promoted gelation of HA-based network precursors (CB[6]-HA and DAH-HA).[135]

4.1.2. Ionotropic gelation

Ionotropic gelation is initiated by the complexation of a cation by several anionic moieties present within two or more polymer chains of the network precursors, thus generating strong reticulation nodes (Fig. 8). This is the case of alginate (Fig. 18) and gellan gum (Fig. 19). Bivalent cations (e.g. Ca^{2+}) are required

to form ionic bonds with at least two oligosaccharide units to create a 3D network. Advantageously, cations triggering the gelation can be added to the bioink using various strategies. Firstly, cations can be dissolved into the bioink before printing thus increasing the viscosity of the hydrogel. Secondly, they can be mixed within a sacrificial ink. Upon contact between the two ink layers, cations diffuse into the bioink containing the network precursors to covalently bind. [115–117] It is often used for co-axial extrusion. Thirdly, the network precursor bioink can be directly printed into a vat or deposited on a bio-paper containing the cations.[136–138] Upon contact, the bioink gelates. It is worth noting that vats are more adapted for extrusion or inkjet, and bio-paper for laser-based printing. Finally, if the printed scaffold is able to keep its integrity long enough without ionotropic cross-linking, it can be cross-linked after by immersion for few minutes into a vat containing the cations. It is generally possible with the addition of another biopolymer to increase the viscosity of the bioink.[8,62,92,139–145]

4.1.2.1. Alginate-based bioinks

So far, about one quarter of the bioinks described in the literature are composed of alginate, alone[92,136] or in combination with other biopolymers. Their popularity can be explained by the simplicity of the ionotropic gelation process, which does require neither chemical reagents, nor specific equipment (e.g. UV irradiation), and by the fact that the network precursor, sodium alginate, is commercially available and cheap.

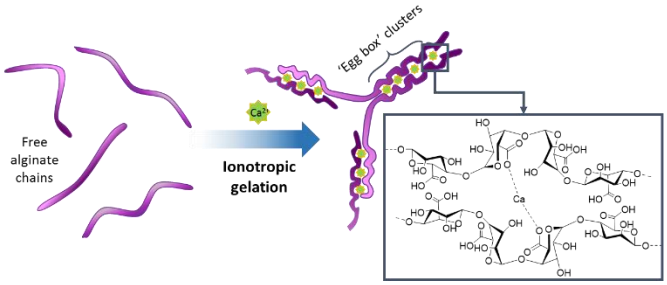

Fig. 18 Ionotropic gelation of alginate.

The calcium cations bind with strong affinity to guluronate units of alginate chains, forming repeated junctions with an identical unit of an adjacent chain. The so-called 'egg box model'[146] is stabilized by evenly distributed ionic bridges formed between carboxylates and the divalent cation (Fig. 18).

Natural extracts are commonly used as additives to alginate to give additional biological properties to the hydrogel. For example blood plasma[8] and dentin extracts, containing growth factors and polysaccharides have been used.[147] Other biopolymers like gelatin[139,140], cellulose derivatives (e.g. nano-fibrillated cellulose[141,142], methylcellulose[116] and ethylcellulose[143]) or a combination of collagen and agarose[144] have also been reported to improve the alginate properties for extrusion printing, mainly viscosity, reinforcing thixotropy and stiffness. Along the same lines, polyvinyl alcohol (PVA)[61,62] has been sometimes added to improve the elasticity of the scaffold and to increase the resolution obtained by extrusion-based printing.

Ahn *et al.*[145] dissolved alginate in a preservation solution containing DMSO and salts like NaCl and $MgCl_2$, commonly used to preserve cell integrity during freezing. It facilitated the bioprinting by extrusion at low temperature (-10 °C). This strategy delivered higher print resolution and scaffold porosity, unfortunately at the cost of lower cell viability.

Many researchers have improved scaffold robustness by creating a composite construct doped with insoluble nano- and micro-structures. For example, nano-hydroxyapatite[63] was added to alginate bioink to allow high throughput printing with laser-induced forward transfer. PLA-sub-micro fibers[148] were added to a cell embedded alginate bioink to improve rheological properties.

Alginate composites are also particularly useful for bone and cartilage engineering. Cho's team[53] used this strategy to print an alginate bioink alternated with PCL layers by extrusion. PCL was used to create a solid framework to improve the stiffness and the stress modulus of the scaffold required for these applications.[95,96] The alginate bioink used in PCL composite scaffolds may also contain other

biopolymers such as gelatin[114] and nanofibrillated cellulose (CELLINK® from Cellink).[93] PCL-alginate alternating layers can also be supplemented by other components such as nano-hydroxyapatite, plasmid DNA, and peptides promoting cell adhesion (e.g. RGD).[60]

From a process point of view, alginate has been used to create vascularized constructs. A coaxial nozzle (Fig. 2A) simultaneously distributed cell-embedded alginate (in the shell), and a calcium chloride solution (in the core). This extrusion process has yielded tubes.[149] PLGA microspheres loaded with the pro-angiogenic drug atorvastatin have also been added inside the 'shell' bioink composed of alginate, collagen and vascular dECM, to create artificial blood vessels.[65] Notably, the reverse process was also performed,[150] i.e. alginate and cells on the core and calcium chloride on the shell, to print hydrogel ribbons with a lower quantity of salts inside the hydrogel and better printing accuracy. At 1% concentration, this hydrogel can also be inkjet-bioprinted directly into a vat of calcium chloride.[137,138]

Grolman *et al.*[151] used a three level co-axial extrusion process developed with microfluidic capillaries. The core of their construct is an alginate bioink, the middle layer is a solution of $CaCl_2$ containing macrophages, and the outer layer is a saturated $CaSO_4$ solution. This process allowed them to co-culture cells to create a micro-environmental tumour model.

4.1.2.2. Gellan gum-based bioinks

Like alginate, gellan gum has the ability to turn into a hydrogel by complexation of calcium ions (Fig. 19). This proceeds at a lower concentration than that of alginate (> 1 wt% for alginate against < 1 wt% for gellan gum), yielding a more elastic material because it is less complexed by calcium.

Lozano *et al.*[105] developed an extrudable bioink based on gellan gum modified with RGD peptides. Carboxylic acid functions of the oligosaccharide were activated by carbodiimide along with sulfo-N-hydroxysuccinimide as auxiliary nucleophile, to react with the N terminal amine of the RGD linear peptide. Ferris *et al.*[152] used gellan gum for droplet ejection and inkjet.

Kesti *et al.*[64] mixed gellan gum, alginate and cells composing a bioink for extrusion in alternation with a pluronic-$CaCl_2$-$SrCl_2$ ink. Interestingly, $SrCl_2$ induces higher storage modulus of the scaffold than $CaCl_2$.

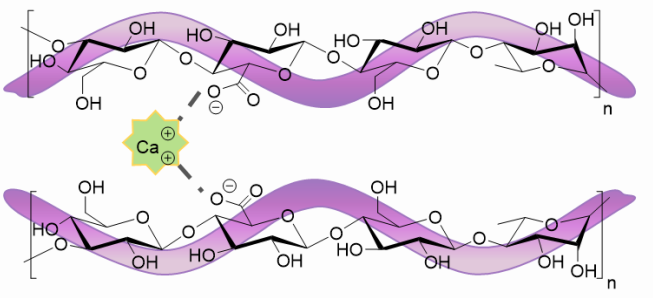

Fig. 19 Ionotropic gelation of gellan gum.

4.1.2.3. Catechol-vanadium-based bioinks

Catechol is known to form complexes with vanadium (vanadyl sulfate) thanks to its ability to form hexavalent species. Lee *et al.*[153] took advantage of this complexation to design a new system of ionotropic gelation. They modified the amino groups of chitosan through reaction with carboxylic acid of catechol. The resulting conjugated biopolymer undergoes ionotropic gelation in the presence of vanadium, producing an extrudable bioink (Fig. 20).

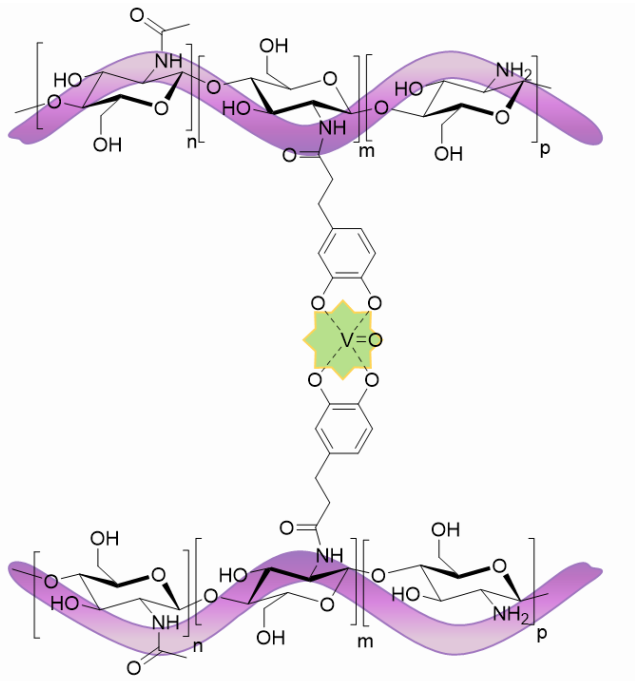

Fig. 20 Catechol-chitosan conjugate complex with vanadyl (IV) ions.[153]

4.2. Covalent assembly (i.e. bioinks-based on chemical hydrogels)

Covalent assembly of network precursors is an irreversible process yielding to chemical hydrogels. Network precursors display mutually reactive functions, ideally in a chemoselective way, to cross-link the 3D network of the bioink. The resulting material will not be able to transform into a liquid but will be degraded in a time-dependent manner, by spontaneous or triggered hydrolysis (e.g. pH, enzymes, UV…). The cells within the bioink are expected to produce their own extracellular matrix, replacing the hydrogel after its degradation. However the scaffold will act as a support during this period, for this reason the degradation rate needs to be controlled as fast, long or even permanent, depending on the targeted application. In fact, non-covalent interactions also contribute to the overall gelation, covalent bonds adding a supplementary degree of stability to the hydrogel.

In the same way as physical hydrogels, the precursor concentration must be high enough to be cross-linked, but more importantly, it is the concentration of reactive functions presented by the bioink components that should be considered for suitable chemical assembly. In other words, the ratio of chemical modifications to unmodified motifs present along the biopolymer backbone is of great importance. To give an idea, covalent bioink networks can be formed by chemical modifications of 10% to 60% residues of biopolymers, and the required concentration of the network precursor to gelate depends on its structure, which is about the same as for physical hydrogels. For synthetic polymers like PEG having reactive groups at both extremities, at least 5 wt% of the network precursor is required to reach gelation. It is possible to modify the physical characteristics of the material such as increasing stiffness, by increasing either the concentration of blocks, or the amount of reactive moieties leading to cross-linkage. Conversely, the more cross-linked the hydrogel, the smaller the pores will be.

Bioinks made from chemical hydrogels enable printing of scaffolds with improved stability and mechanical properties, but they are not straightforward to use as physical hydrogels. Firstly, most of the commonly used network precursors must be chemically modified before preparation of the bioink to display suitable reacting groups. Secondly, special attention must be paid to the biocompatibility of the reticulation reaction itself. All the reactants, catalysts, solvents and products need to be non-toxic, as well as the reaction conditions (temperature, pH), which may also require specific printers (e.g. a heating system, a UV lamp for curing). These factors limit the available chemistries to a handful of cell-friendly reactions. All examples cited in this chapter are brought together in Tables 3 and 4 (Chemical gelation-based bioinks and Complex bioinks).

4.2.1. Chemical modification of precursors

As already stated, chemical cross-linking necessitates prior modification of the network precursor, whether they are biomacromolecules or synthetic polymers. Many chemical modifications[154] have been proposed, but this review will only focus on those that were successfully used for 3D-bioprinting. The most popular chemical modification of bioink network precursors is the introduction of vinyl groups. Such unsaturated moieties are prone to many bio-orthogonal reactions, including Michael addition, chain-growth photo-polymerization and step growth polymerization (see 4.2.2). Acrylate and methacrylate moieties are the most important class of vinyl acceptors. The second most commonly encountered functionalizations are thiol incorporation, as partners of unsaturated moieties for Michael additions, or to form disulphide bridges.

Introduction of acrylate derivatives

The functionalization of biopolymers is preferentially done on amine and alcohol functions of the macromolecule, using methacrylic anhydride in aqueous conditions (Fig. 21A and 21B).[99,102,155–158] The epoxide precursor, i.e. glycidyl methacrylate (GMA), is also reported, to react with primary amines in the presence of LiBr to yield secondary amino groups (Fig. 21C).[159] Functionalization has been performed on the backbone of proteins such as

gelatin and silk fibroin,[159] oligosaccharides including hyaluronic acid,[157] and on the extremities of linear or branched PEG. A wide range of methacrylated, dimethacrylated, and diacrylated (Fig. 22) PEGs of various sizes are commercially available. They can be prepared from non-functional PEGs, using the same types of reaction as those used on biopolymers (e.g. methacrylation with methacrylic anhydride in DCM in the presence of triethylamine[160]).

Introduction of alkenes

Simpler alkene groups constitute an alternative to acrylates, especially for thiol-ene chemistry. They are preferentially used for cross-linking between two different species. Thiol-ene is a step-growth polymerization process, whereas acrylate polymerization is a chain polymerization, meaning that one may expect to exert better control of the cross-linking between different species, and of the number of network precursors involved in the chain. The polymerization reaction can happen with either a thiolated biopolymer or a thiolated bi-functional linker like dithiothreitol (DTT).

Allyl groups were introduced by reaction of allyl glycidyl ether with primary amines. This has been achieved with gelatin in basic medium at 65 °C for 24h (Fig. 21D).[161] Alternatively, amino norbornenes may react with carboxylic groups of biopolymers activated by carbodiimide (Fig 21E). This has been performed on the backbone of alginate.[106]

Introduction of thiols

Thiols are attractive functional groups for cross-linking bioinks. As already stated, they are partners of thiol-ene reactions and Michael addition, but can form by oxidation, intermolecular disulfide bridges between network precursors.

Sulfhydryl groups have been introduced through bi-functional symmetrical disulfides. They first yield intra- or inter-molecular bridged species, which are further converted into sulfhydryl modified polymers by reduction. As an example, the hydrazine function of 3,3'-disulfanediyldi(propanehydrazide) has been substituted in the carboxylic acid functions of HA activated by carbodiimide (Fig 21F). After reduction of disulphide bonds with DTT, a sulfhydryl-containing HA cross-linkable by oxidation was obtained.[97]

Introduction of other types of functional groups

Bio-orthogonal reactions are required to avoid unwanted reactions of the network precursors with other biomolecules present in the buffer (e.g. growth factors, nutriments) or with the proteins on the surface of the cells. Such reactions necessitate functional groups, which are not naturally present in biomolecules such as vinyl moieties. Aldehydes and hydrazides may react together through hydrazine ligation, which has been used for HA cross-linking. Adipic acid dihydrazide was coupled to HA to install a hydrazide function on the backbone. It is important to note that this functionalization should proceed carefully to avoid unwanted premature formation of already cross-linked or cyclic species (Fig. 21G).[162] Aldehyde functionalized HA has been prepared by controlled oxidation of cyclic saccharides of the backbone with sodium periodate (Fig. 21H).[162]

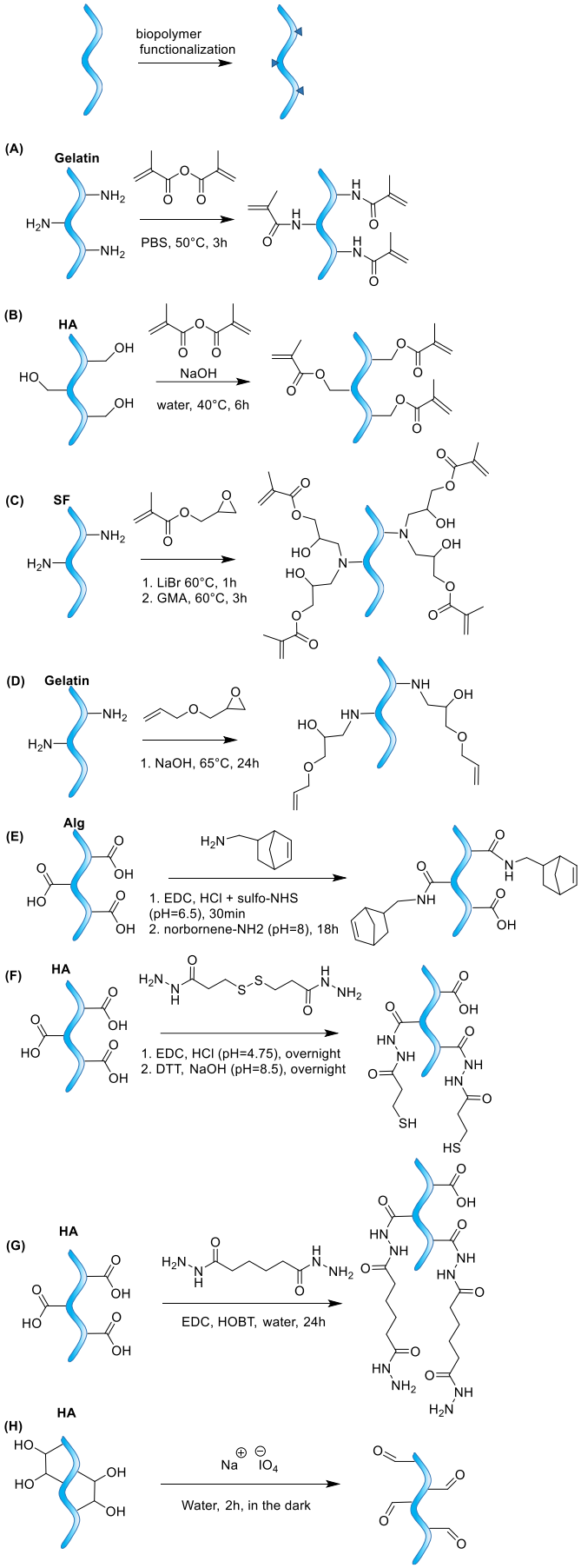

Fig. 21 Chemical modifications of biomacromolecular network precursors: (A) gelatin methacrylation; (B) HA methacrylation; (C) silk fibroin methacrylation; (D) gelatin allylation; (E) alginate functionalization with norbornene; (F) HA thiol functionalization; (G) HA hydrazide functionalization; (H) HA aldehyde functionalization.

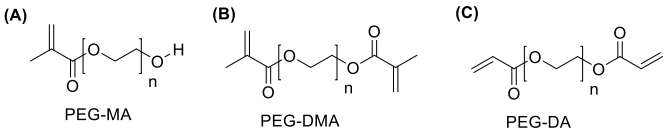

Fig. 22 Functionalized PEGs: (A) polyethylene glycol methacrylate; (B) polyethylene glycol dimethacrylate; (C) polyethylene glycol diacrylate (PEG-MA, PEG-DMA and PEG-DA, respectively).

Chemical cross-linking reactions used for bioink preparation can be sorted between UV-promoted reactions (chain growth polymerization of acrylates with photo-initiator and radical thiol-ene cross-linking), bio-orthogonal chemical reactions (Michael addition, hydrazide ligation and Schiff base reaction) and enzymatic cross-linking.

4.2.2. Photo cross-linking

Cross-linking and polymerization can be initiated by UV irradiation thanks to the presence of a photo-initiator in the bioink. Of course, UV irradiation is the fundamental principle of stereolithography printers, but most 3D extrusion and inkjet 3D bio-printers include UV cross-linking devices. The availability of such devices has made this mode of polymerization very popular. Moreover, photo-catalysed gelation of bioinks is very fast (a few seconds), and the liquid bioink containing cells can be gelated right after the exit of the print head (extrusion nozzle or inkjet). Alternatively, UV irradiation can take place on top of the printed scaffold. This second option is only possible when bioinks are viscous enough not to flow immediately after extrusion.

Perhaps the main drawback of photo cross-linking comes from the toxicity of photo-initiators (PI). Only a small number of them can be used at low and controlled concentrations in water (see 4.2.2.3.). In some cases, the toxicity has been reduced by

washing the scaffold after printing. To perform polymerization, different strategies are envisaged. For stereolithography and digital light processing, the photo-initiator is suspended in the bioink. Reticulation takes place where the light beam hits the solution, and the shape of the scaffold is made by superposition of layers.

For other bioprinting technologies, the photo-initiator is solubilized in the bioink or a sacrificial ink, and UV curing is performed either during or after printing.

The two main mechanisms of photo cross-linking are chain growth photo polymerization and step growth polymerization, using two partners, an alkene and a thiol.

4.2.2.1. Chain growth polymerization of acrylated polymer-based bioinks

Chain growth photo polymerization is performed by radical polymerization on the kinetic chain (chain in expansion during the polymerization). It has been used on acrylates and methacrylates, and requires only one type of functional group. This means that a single type of acrylated precursor can be used as a bioink. Alternatively, any other component can be part of the cross-linked network insofar as it is acrylated (Fig. 23A). This interesting feature means that a wide range of hydrogels with various physical specificities (viscosity, elasticity, pore size, etc.) can be obtained by varying the nature of the precursors (e.g. gelatin and PEG), and the ratio of each species (e.g. 1/1, 1/10, etc.).

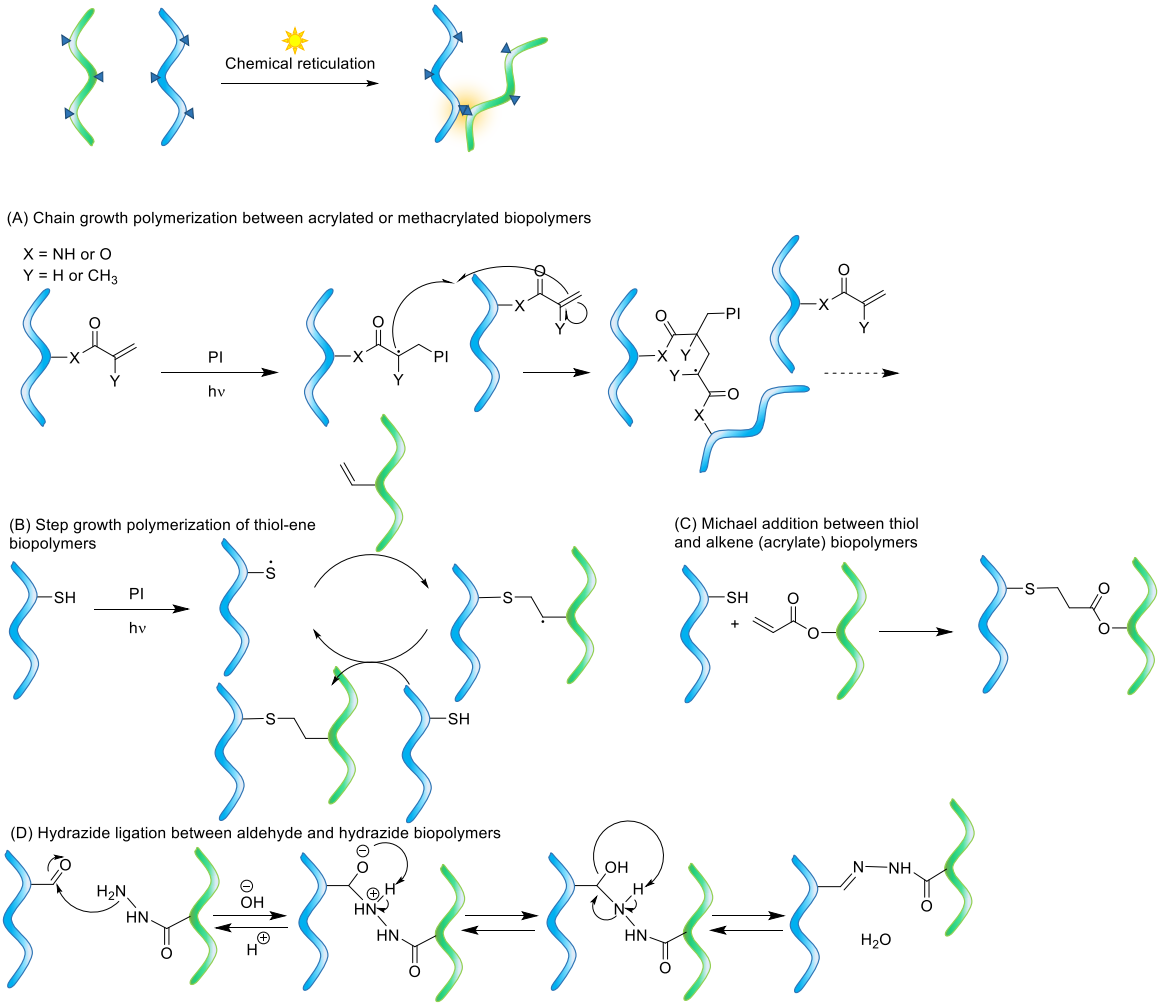

Fig. 23 Photo cross-linking reactions used in bioinks: (A) Chain growth polymerization between acrylated and methacrylated species; (B) step growth polymerization (radical thiol-ene reaction); (C) Michael addition (thiol-acrylate reaction); (D) hydrazide ligation (aldehyde-hydrazide reaction).

The most common acrylated network precursor is the commercially available methacrylated gelatin (Gel-MA, Fig. 21A). 20% to 95% of gelatin repetition units can be modified by acrylate, depending on the amount of equivalents of reagents used to functionalize gelatin. It has been printed by nanoliter droplet deposition[55] at about 5 % w/v concentration, and printed by stereolithography or DLP, using a vat at 10 to 30 % w/v concentration.[163] With a 10 % w/v concentration, it can be extruded.[92] The gelation time depends on the PI used and its concentration (from less than one minute to a few minutes).

As explained above, Gel-MA can be used either alone for extrusion or in association with other modified macromolecules such as methacrylated-hyaluronic acid (HA-MA, Fig. 21B).[157] Di Bella *et al.*[164] also used a 2:1 Gel-MA/HA-MA mixture as an ink to load a custom-made extrusion bio-pen. One cartridge was filled with the ink and another with the cell embedded ink, both delivered at the same time. They used this pen to directly fill a defect present on a sheep knee.

It is also possible to add non methacrylated compounds like silk fibroin[155] to print by digital light processing, or gellan gum embedding PLA-micro carriers containing cells for extrusion.[165] Chimene *et al.*[102] developed a multicomponent bioink (called NICE, or Nano-engineered Ionic-Covalent Entanglement) composed of Gel-MA, κ-carrageenan and 2D-nanosilicates. By extrusion and UV cross-linking, they obtained constructs with high fidelity, stiffness and elasticity. Yin *et al.*[156] extruded a Gel-MA and gelatin bioink. The specificity of this bioink resides on a two-step cross-linking protocol consisting of fast and reversible thermo cross-linking of gelatin, and irreversible photo cross-linking of Gel-MA. It allowed better printing accuracy and fidelity with good cell viability, than using them alone.

Liu *et al.*[166] used a co-axial extrusion process to simultaneously print a Gel-MA solution containing cells and $CaCl_2$, and alginate sheath. Both ionotropic gelation and UV cross-linking occurred, yielding micro-fibers. Zhu *et al.*[99] also used co-axial extrusion of a core bioink made out of Gel-MA, alginate and gold nanorods coated with Gel-MA, and a calcium chloride shell solution. These gold nanorods allowed them to improve the conductivity of the scaffold, and to reach an efficient electrical coupling between adjacent cardiac cells, inducing better spreading and organisation, to perform cardiac repair. The extrusion of a Gel-MA shelf has also been commonly used with sacrificial pluronic core with PDMS[98] or alginate, and 4 arms PEG-tetra-acrylate (PEGTA)[167] mixed with the Gel-MA. However, after UV-curing, it has been possible to use an EDTA vat, which complexes calcium ions, to remove the liquefied alginate leaving to a vascularized construct.

PEG derivatives are also a common class of UV cross-linkable precursors. Bi-functional PEGs (e.g. PEG-DMA, PEG-DA, Fig. 22) have been used for inkjet printing.[168,56]

Composite bioinks can be prepared by also mixing non-acrylated components, molecules and particles. Peak *et al.*[169] mixed disk-shaped 2D nanosilicates and PEG-DA to obtain a colloidal bioink that could be UV cross-linked, with self-healing properties. Gao *et al.*[101] inkjet-printed a bioink made out of PEG-DMA, hydroxyapatite and nanoparticles of bioactive glass (BG 45S5). These two different osteogenic factors improved cell differentiation in osteoblasts, resulting in a scaffold with a higher compressive modulus, which is essential for bone tissue engineering.

As for Gel-MA based bioinks, other acrylated compounds can be covalently incorporated in the network to afford additional properties. Xu *et al.*[170] used a triblock copolymer of diacrylated PCL-PEG-PCL as a major component of their extruded bioink (Fig. 24) that reacts as other diacrylated compounds (Fig 18A). It can also be used to introduce RGD sequences (using RGD-PEG-DA monomer), which enhance cellular adhesion.[59] There is no limitation in the number of different acrylated components that can be combined in the bioink. For example, an enzyme-degradable bioink, printed by inkjet, was prepared by mixing PEG-DMA, acrylated RGD sequences and acrylated MMP-sensitive peptide sequences (e.g. GCRDGPQGIWGQDRCG).[57,58]

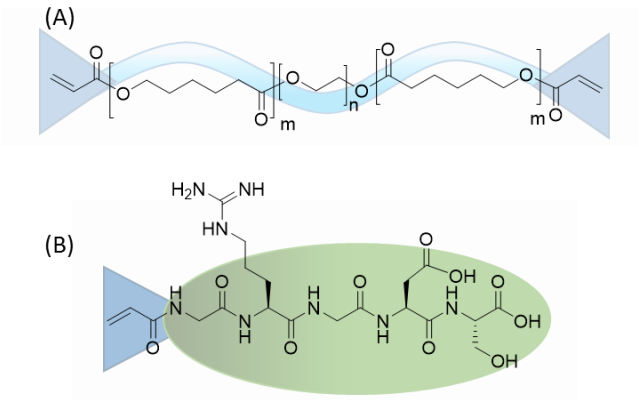

Fig. 24 A) PEG-PCL-DA bioink,[170] and (B) acrylated-RGD.[57,58]

Combination of PEG and gelatin, two of the most popular acrylated precursors, has been investigated for stereolithography[171] or extrusion.[172]

The only other reported example of acrylated network precursors as bioink components, besides gelatin and PEG, is methacrylated silk fibroin (Fig. 21C), which was successfully used as a light processing 3D printable bioink precursor.[159]

4.2.2.2. Thiol-ene radical photo-polymerization-based bioinks

From a mechanistic point of view, the thiol-ene radical polymerisation reaction is very different from the chain growth polymerization. Indeed, it requires two distinct partners: a nucleophile acceptor (alkene), and a thiyl radical obtained by activation of a thiol using a PI under UV irradiation (Fig. 23B). Strictly speaking, the network is established by repetition of multiple cross-linking and not by the polymerization of the same monomer.

This process has been described by reaction between allylated gelatin (GelAGE, Fig. 21D) and DTT (Dithiothreitol) as cross-linker, for extrusion and stereolithography.[161] With this same reaction, norbornene functionalized alginate (Fig. 21E) can be cross-linked with PEG-dithiol.[106] Thiol functionalized RGD sequences were also added to improve bioink cell adhesion. Stichler *et al.*[97] developed a bioink with thiol-HA (Fig. 21F) and poly(allyl glycidyl ether-co-glycidyl) (P(AGE-co-G). They successfully extruded this bioink in alternation with PCL layers.

4.2.2.3. UV photo-initiators

A limited number of photo-initiators (PI) have been used for bioprinting (Fig. 25). This can be explained by the cytotoxicity and the poor water solubility of most of them. PIs are mostly used at concentrations ranging from 1.7 to 0.01 mM depending on their respective toxicity. The most used is Irgacure 2959 (I2959),[10,55,57–59,92,97,98,161,162,165,168] ([4-(2-hydroxyethoxy)-phenyl]-2-hydroxy-2-methyl-1-propane-1-one, Fig. 25A), which absorbs at 257 nm. Lithium phenyl(2,4,6-trimethylbenzoyl)phosphinate (LAP, Fig. 25B) absorbs at 375 nm and is less toxic than Irgacure.[106,159,170] Eosin Y (2′,4′,5′,7′-tetrabromofluorescein disodium salt, Fig. 25C) absorbs at 514nm (blue visible light), which induces less oxidative stress for cells.[155,171] It is worth noting that only eosin Y and I2959 have been FDA-approved to date.

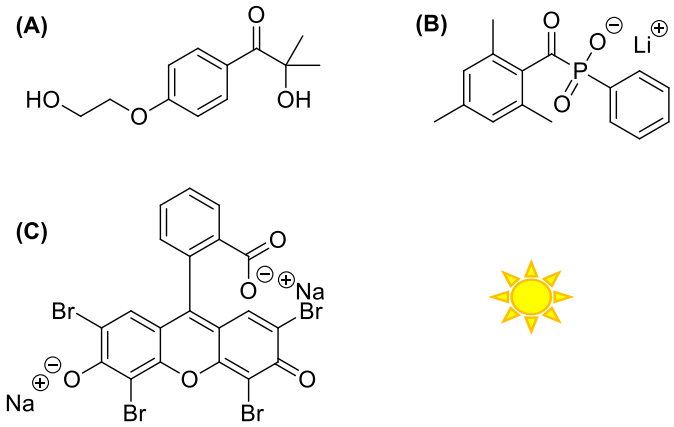

Fig. 25 Common photo-initiators used in 3D bioprinting: A) Irgacure 2959; B) LAP; C) Eosin Y.

4.2.3. Chemical cross-linking

Needless to say, some well-known bioconjugation 'click' reactions have been used for bioink reticulation. Indeed, they take place in water, in a highly efficient and in ideal conditions in a bio-orthogonal manner. Unlike acrylate polymerization, such reactions proceed between two different types of mutually reactive groups (e.g. aldehyde and hydrazide, maleimide and thiol). This implies that a mixture of two (or more) different precursors, each one bearing a different reactive moiety, must be used to form the network. The combination potential gives considerable freedom in the design of hydrogels with different physical properties, depending on both the ratio of each monomer and on the amount of cross-linking. Surprisingly, despite its immense popularity,

Huisgen 1-3 dipolar cycloaddition has not been exploited in bioprinting so far, probably due to the toxicity of the copper catalyst. Even its metal-free counterpart, strain promoted alkyne-azide cycloaddition (SPAAC), has not been used until now for bioink preparation. This is not the case for thiol-based ligation methods. Strictly speaking, thiol-based conjugation is not bio-orthogonal as proteins present in the bioink (i.e. on the cell surface or as soluble factors) contain cysteine residues, which could react with sulfhydryl containing compounds, even when most cysteines are involved in disulfide bridges in proteins. However, this chemistry is still extensively used in bioinks, either with simple vinyl groups or with acrylates, which are easier to prepare.[173–176] Non-radical thiol-ene chemistry (i.e. Michael addition) generates no side products and is highly selective. The addition can be nucleophile-catalysed, but in bioinks the medium cannot be too basic, pH should be kept close to neutrality. However, it is important to realise that the reaction takes a few minutes to start, and if the viscosity is not sufficient, the bioink needs to be cross-linked enough before to be printed or mixed with a stiffer component.

Skardal *et al.*[177] developed a Michael addition-based bioink including two network precursors: a thiolated HA (synthesised as previously described Fig. 22F) and a 4-arms PEG bearing an acrylate moiety at each of its extremities (named TetraPAc8 or TetraPAc13 depending on the size of the PEG, Fig. 26). Notably, the resulting chemical cross-linked hydrogel was also stabilised by non-covalent interactions between hyaluronic acid chains. This bioink was printed by micro-extrusion, after 30 minutes of cross-linking, using micro capillary tubes instead of regular syringes. Using agarose hydrogel as a sacrificial ink, cellularized vessel-like constructs were prepared.
Classical maleimide-thiol Michael addition has also been exploited to create bioinks. Yan *et al.*[178] used thiolated gelatin soaked for 15 minutes in a solution containing bi-functional maleimide PEG, to yield a network cross-linked through thioether bonds. Notably, amphiphilic fibril-forming peptides (acetyl-VVAAEEIKVAV and acetyl-VVAAEE) derived from laminin sequences have been also added in the bioink to facilitate a non-covalent gelation at 4 °C and improve the cell adhesion. The initial physical network was strengthened by chemical cross-linking at 37 °C, and induced a higher cell viability because of the peptides.

Aldehyde-hydrazide ligation yields hydrazone linkage in a fully chemoselective manner. This reaction proceeds by addition of the hydrazide on the aldehyde with water formation (Fig. 23D). For example, HA-based two-component bioinks have been 3D-printed by extrusion, after 2 hours of cross-linking. Hydrazone linkages were formed between HA modified with hydrazide groups and HA displaying aldehyde functions (Fig. 21 G and H).[162]

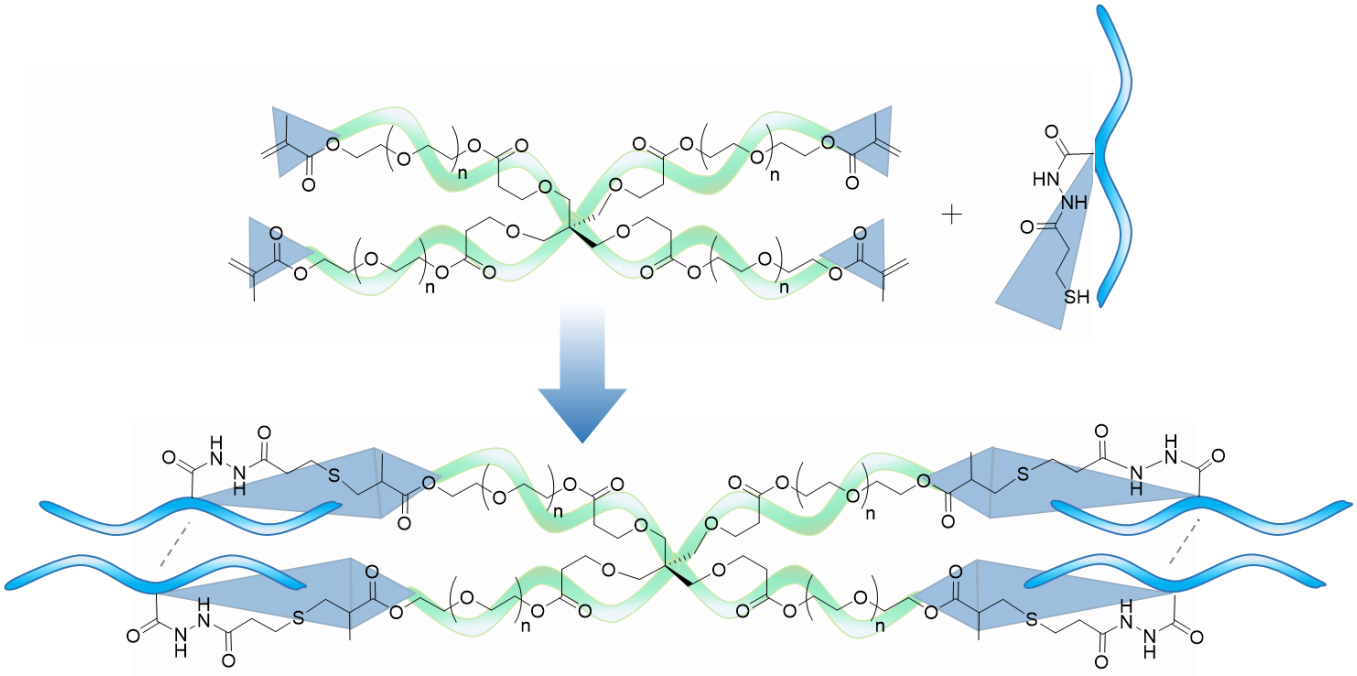

Fig. 26 Bioink formation between thiol-HA and TetraPAc.[177]

The aldehyde function may also react with amino groups to form an imine via a Schiff-base reaction (Fig. 23D), by the same mechanism than hydrazine ligation, typically under basic conditions. This reaction is reversible by acidification, however the pH of transition depends on the stability of the resulting imine-containing compound. This mean that for some compounds the reaction can be done at physiological pH. Du *et al.*[179] extruded a mixture of an oxidized dextran functionalized with aldehyde moieties and gelatin. The aldehyde moieties reacted with amino groups of gelatin yielding imines at physiological pH (from 6 to 8) (Fig. 27). It should be stressed that gelatin itself forms a physical hydrogel and helps to the stability of the printed scaffold. In addition of its pH sensitivity, the mixture is also thermo sensitive thanks to gelatin. At pH 7.4 and 37 °C, gelation happens within 20 minutes, but occurs in only 5 minutes at 18 °C. Indeed, the low temperature induces a phase separation, which corresponds to the colloidal form of gelatin.

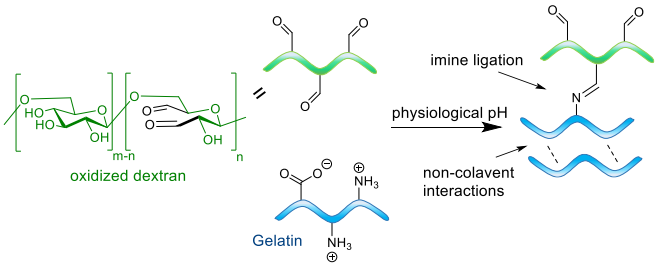

Fig. 27 Bioink formation between oxidized dextran and gelatin.[179]

4.2.4. Enzyme-driven gelation

Enzymes are attractive auxiliaries to perform chemical cross-linking in cell-friendly conditions, with a bio-orthogonal control of the gelation process, and high specificity. They can be used either to generate a new reactive functional group on a network precursor (e.g. aldehyde) that may subsequently react with another mutually reactive moiety, or to directly cross-link the components of the bioink (e.g. forming amide bonds). However, the use of enzymes excludes excessive harsh conditions (high temperature, solvents or denaturing compounds), which are less permissive than for cell embedding. A few studies have been published on enzymatic gelating bioinks to date. Indeed, this is not a straightforward task, as specific

substrate sequences recognized by enzymes must be introduced within the precursors. Enzymes are also expensive materials and their production, from animal extracts and recombinant bacterial origin, is not easily compatible with human body implantation. These issues may constitute a barrier to the widespread use of enzymatic cross-linking for 3D printing.

4.2.4.1. Transglutaminase gelation

Transglutaminase catalyses transamidification between lysine and glutamine side chains (Fig. 28), yielding an inter chain amide bond. Dai *et al.*[180] used this transglutaminase (1 wt%) to generate covalent cross-linking between gelatin macromolecules. In a similar fashion to other chemical bioinks able to cross-link, a physical hydrogel precursor such as alginate that has been incubated in a $CaCl_2$ vat, was used as an additional component of the bioink to facilitate the extrusion process, and to maintain the integrity of the printed scaffold, while enzymatic cross-linking reaction proceeded.

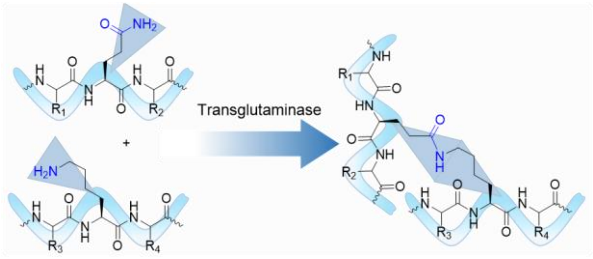

Fig. 28 Transglutaminase cross-linking.

4.2.4.2. Enzymatic activation of gelation

In a different strategy, enzymes can be used to generate reactive groups on the backbone of network precursors (e.g. biopolymers or synthetic polymers), which may afterwards react with other moieties, like in chemical cross-linking (see 4.2.3).

Arai *et al.*[181] exploited the reactivity of the phenoxy radical generated from phenols by horseradish peroxidase (HRP, Fig. 29). These radicals react with each other to form oxydibenzene. These reactions allowed gelatin and phenolic-modified alginates polymerization. The second one was synthesised according to the same process than norbornene-functionalized alginates, but with tyramines as second reactants (Fig. 21E). Once again, alginate $CaCl_2$-induced ionotropic gelation contributed to the stability of the inkjet-printed scaffold during the enzymatic reaction.

Monoamine oxidase B (MOA-B) specifically transforms benzylamine into benzaldehyde through a benziminium intermediate. Consequently, Wei *et al.*[182] have used MOA-B to turn bifunctional PEG terminated by 4-aminomethyl benzoic acid into its di-benzaldehyde counterpart, which reacted as a bifunctional cross-linker with primary amines of glycol chitosan or gelatin yielding Schiff base linkages (Fig. 30). Unfortunately, the MOA-B-catalysed reaction generates hydrogen peroxide, which is toxic for cells. Catalase was added to convert H_2O_2 into water and dioxygen, thus improving cell viability.

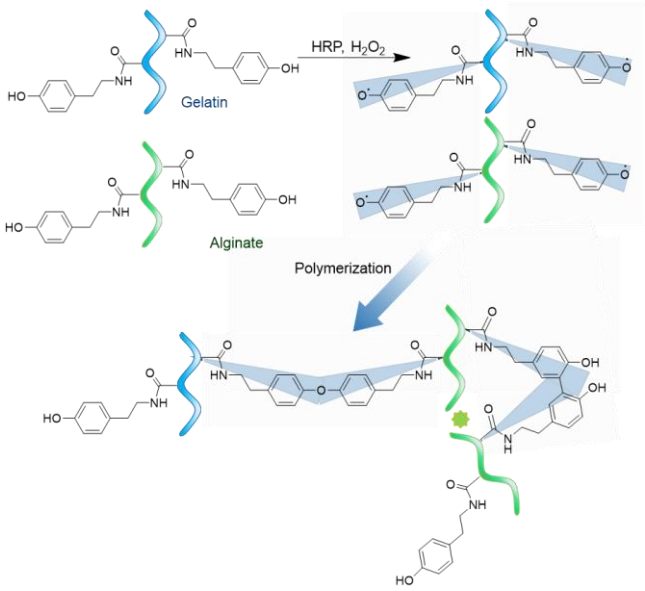

Fig. 29 Enzymatic oxidation with HRP.[181]

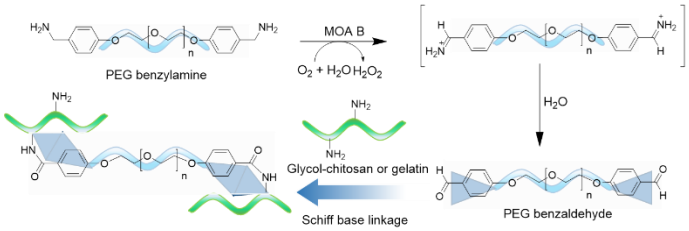

Fig. 30 Mechanism of bioink gelation using MOA-B and Schiff base cross-linkers.[182]

4.2.4.3. Thrombin/Fibrinogen bioink

The last example of enzyme-based gelation of bioinks was directly inspired by the clotting of fibrinogen by thrombin, leading to fibrin fibers (Fig. 31).[67] Fibrinogen is a hexameric glycoprotein, which is cleaved by thrombin at the N-terminus part of its alpha and beta chains (giving fibrinopeptides side products) lead to self-assembly between its D and E domains, turning it into fibrin fibers by polymerization.

Cui and Boland[183] proceeded by direct biomimicry using a solution of thrombin (50 unit/ml) with cells. This bioink was inkjet-printed on a support (i.e. bio-paper) constituted of fibrinogen. The clotting reaction occurred at the interface of the bio-paper and the bioink. They used a low viscosity solution containing the enzyme and cells thus limiting this strategy to inkjet printing of thin constructs. Accordingly, Xu *et al.*[94] combined fibrinogen/thrombin with collagen to print cellularized layers alternated with layers of PCL-pluronic by inkjet printing. Zhang *et al.*[82] used two bioinks with the same composition (composed of fibrinogen, gelatin and hyaluronic acid), with two different types of cells. These bioinks were viscous enough to be extruded with polylactic-co-caprolactone (PCL-PLCL) layers to perform a co-culture, after incubation in a thrombin solution vat, to cross-link bioinks.

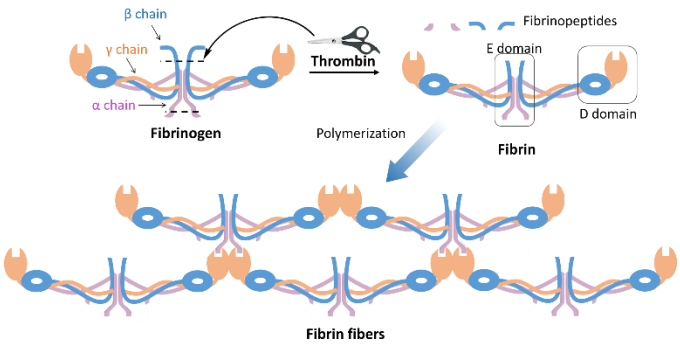

Fig. 31 Thrombin-driven fibrinogen polymerization (adapted from *Biochemistry* 7th Edition, 2012, W. H. Freeman and Co.).

Fibrinogen and thrombin have been printed in different bioinks, meaning that the enzyme will migrate through it or the printed scaffold is placed in a vat containing the enzyme, as a post-printing process.

Skardal *et al.*[117] printed a bioink made out of fibrinogen, collagen and cells, in alternation with layers of a thrombin solution, directly into a wound on the back of mice, by inkjet process. Kolesky *et al.*[91] co-extruded a cell-embedded fibrinogen-gelatin bioink with a core of pluronic-thrombin sacrificial ink. The enzyme diffused from the core to the outer layers containing the fibrin, yielding artificial vessels after removal of the Pluronic.

5. Conclusion and prospects

Access to 3D-bioprinting for laboratories has never been so easy, thanks to a range of affordable 3D printers, which all claim cell-handling compatibility.

The 3D bioprinting popularity is growing along with the well-documented utilization of a handful of robust, commercially available, 'basic' hydrogels including gelatin, HA, alginate, which may embed cells during the printing process.

Physical hydrogels based on biopolymer network, used as single components and as mixtures, dominate the field. Their use for bioprinting does not require any chemistry. However, when long-term applications or more demanding mechanical properties are targeted, the development of chemical hydrogels is necessary. Even in this case, the use of physical hydrogels as additional components is appreciated to alleviate the lack of stiffness after the printing process, and to keep the integrity of the scaffold while the chemical reaction proceeds.

The majority of the chemical bioinks used are photo-polymerized, owing to the compatibility this process offers, with many printers, many network precursors and cells.

A relatively small repertory of cross-linking reactions including thiol-ene and acrylate polymerization, is used. For the organic chemist, there is a lot of scope for imagination or simply for applying efficient bio-orthogonal ligation procedures to the field of bioprinting.

Whatever the application chosen, from vascularized tissues, organs and scaffolds for tissue engineering, to disease models and chips for high-throughput

screening, the trend is towards increasing complexity of the printed construct. Indeed, the ultimate goal is to reproduce the hierarchical micrometric organization of tissues as well as their diverse mechanical properties. The challenge is taken up via two approaches including (i) combination of several printing techniques to sequentially construct bulk material and small, highly organised structures like vessels, with higher resolution, and (ii) addition in the scaffold of different materials such as plastic supporting layers, sacrificial ink, and embedded fibers or nanoparticles in the bulk, yielding composite bioinks matching the targeted properties. The other scientific challenge is the creation of biologically active scaffolds that not only pass the test of 3D printing and guarantee the survival of printed cells, but also enable cells to grow, differentiate, migrate and be organized into relevant biological structures. A lot of effort has been devoted to this field, essentially by adding bioactive compounds including signalling peptides, growth factors, drugs whose release and availability in the hydrogel could be triggered by various release systems (e.g. porous particles, micelles, sensitive linkers). Covalent modifications of the hydrogel network find here all their significance, either giving permanent cell-binding properties to the network or enabling the controlled and sustained release of a drug via a system that can be targeted. For tissue-engineering applications, enzyme-sensitive degradation sequences can be inserted into the covalent hydrogel matrix to enhance the degradation of the artificial scaffold and its replacement with the newly synthesized ECM. Once again, bio conjugation chemistry is here, one of the major players.

Bioprinting is still in its infancy, and the first phase has been mostly occupied by printer's technological optimization, and development of bioink formulations suitable for each printing technique using combinations of well-known polymers and cross-linking chemistries. The next frontier that must be crossed is the development of universal, multifunctional and tunable bioinks that can be mixed together to enable a full range of biological and mechanical properties of tissues to be mimicked, from bone to brain and vessels. The density of cross-linkers and the length and geometry of network precursors define the resulting physical characteristics of the material. When an in-human 3D printed tissues is envisioned, one must move away from using animal extracts as bioinks. Synthetic biomolecules including proteins and oligosaccharides should be preferred to afford closer analogues of natural tissues. These synthetic biomimetic components should allow chemical cross-linking and/or present self-assembling properties to generate a suitable hydrogel network, while keeping their bioactivity. Finally, the universality of the system, i.e. the same type of chemistry for assembly applied to all the different network precursors and additional components, will alleviate the problem of integration between layers, and simplify the overall conception of a multi scale non-homogeneous scaffold printed with different 3D bio-printers.

Table 2 Physical bioinks described in the literature (NA = not assayed, NS = not specified)

GELATION PROCESS	NETWORK PRECURSOR	NETWORK PRECURSOR CONCENTRATION	OTHER COMPONENTS	POST PRINTING PROCESSING	PRINTER TYPE	CELL TYPE	CELLULAR CONCENTRATION	CELLULAR VIABILITY	IN VIVO ASSAYS	APPLICATION	REF.
aggregation	agarose (type VII)	2%			extrusion	bone marrow derived mesenchymal stem cells (BM-MSCs)	$20*10^6$ cells/ml	90% after printing		cartilage tissue engineering	92
aggregation	agarose (ultra-low-gelling-temperature)	1.3-1.5% w/v	Fmoc-dipeptide solution (1mM) + collagen (15 µg/ml)	printing into an oil vat	droplet-based (piezoelectric generator)	HEK-293T cells and ovine mesenchymal stem cells (MSCs)	$5\text{-}15*10^6$ cells/ml	90% after printing		platform	124
aggregation	hyaluronic acid + methylcellulose	2.0 wt% and 5-9 wt%			extrusion	sheep MSCs	NS	>75% after printing		platform	184
ionotropic	catechol-conjugated-chitosan	2 wt%	vanadyl ion solution (50µM)	printing into media with serum (FBS, 5-25%)	extrusion	L929 cells	$10*10^6$ cells/ml	90% after printing		platform	153
ionotropic	endotoxin-free low-acyl gellan gum	1% w/v			droplet ejection + inkjet	mouse C2C12 cells and PC12 cells	$0.2\text{-}2*10^6$ cells/ml and $1\text{-}6*10^6$ cells/ml	95% after printing		platform	152
ionotropic	e + sodium alginate	6 and 5 wt%		incubation in $CaCl_2$ solution after printing	extrusion	porcine aortic valve interstitial cells (AVIC) or Human aortic root smooth muscle cells (SMC)	$10*10^6$ cells/ml	>85% after printing		aortic valve conduit construction	139
ionotropic	gelatin+ sodium alginate	12% and 2.4% w/v		incubation in $CaCl_2$ solution after printing	extrusion	mouse epidermal stem cells (ESCs)	$1*10^6$ cells/ml	>90% after printing		platform	140

ionotropic	Gellan gum-RGD (core)	0.5% w/v	$CaCl_2$ solution (shelf)		co-axial extrusion	primary mouse cortical neurons	$1*10^6$ cells/ml	>70% after 2h		representation of 3D brain-like structure	105
ionotropic	nanofibrilated cellulose + sodium alginate	1.5-2 % w/v and 1-0.5% w/v	mannitol (4.6%)	incubation in $CaCl_2$ solution after printing	extrusion	human induced pluripotent stem cells (hIPSCs)	$20*10^6$ cells/ml	good (non quantitative)		cartilage repair	141
ionotropic	nanofibrillated cellulose / sodium alginate (NFC-A) bioink (from CELLINK AB)	92% v/v from commercial concentration		incubation in $CaCl_2$ solution after printing	extrusion	hBMSCs)and human nasal chondrocytes (hNCs)	$10*10^6$ cells/ml	NA	female Balb/c nude mice	cartilage repair	142
ionotropic	sodium alginate	3.5%	$CaCl_2$	incubation in $CaCl_2$ solution after printing	extrusion	BM-MSCs	$20*10^6$ cells/ml	80% after printing		cartilage tissue engineering	92
ionotropic	sodium alginate	8wt%	collagen or agarose (0.3 wt%)	incubation in $CaCl_2$ solution after printing	extrusion	rat primary chondrocytes	$10*10^6$ cells/ml	>80% after printing		cartilage tissue engineering	144
ionotropic	sodium alginate	2-1% w/v	insoluble dentin proteins or soluble dentin molecules		extrusion	mouse odontoblast-like cells (OD21) and stem cells from the apical papilla (SCAP)	$2*10^6$ cells/ml and $0.6*10^6$ cells/ml	>70% after 1 day		regenerative dentistry	147
ionotropic	sodium alginate	3% w/v	laponite (3% w/v) + methylcellulose (3% w/v)	incubation in $CaCl_2$ solution after printing	extrusion	hMSCs expressing hTERT (human telomerase reverse transcriptase)	$0.5*10^6$ cells/ml	70% after 1 day		bone tissue engineering	143
ionotropic	sodium alginate	2.5%	2.5% hydroxyapatite + 1% polyvinyl alcohol (PVA) + 0.15% Na_2HPO_4 +, 0.20% $CaSO_4$		extrusion	mouse calvaria 3T3-E1 (MC3T3) cells	$0.01*10^6$ cells/ml	80% after printing		bone tissue engineering	61

ionotropic	sodium alginate	2.5%	2.5% hydroxyapatite + 1% polyvinyl alcohol (PVA) + 0.15% Na_2HPO_4 +, 0.20% $CaSO_4$	incubation in $CaCl_2$ solution	extrusion	MC3T3 cells	$1*10^6$ cells/ml	>90% after 1 day	bone tissue engineering	62
ionotropic	sodium alginate	3wt%	cell-freezer solution (Gen-1001) $CaCl_2$	incubation in $CaCl_2$ solution after printing	extrusion (low-temperature processing method (DLTM))	osteoblast-like cells MG63, CRL-1427 and hMSCs	$1*10^6$ cells/ml	70-80% after printing	platform	145
ionotropic	sodium alginate	1wt%		printing into $CaCl_2$ solution	inkjet	NIH 3T3 mouse fibroblasts	$5*10^6$ cells/ml	90% after printing	vascularized tissue engineering	138
ionotropic	sodium alginate	0.8-1%		printing into $CaCl_2$ solution	inkjet (self developed)	HeLa cells	$6*10^6$ cells/ml	NA	platform	137
ionotropic	sodium alginate	2wt%	EDTA human blood plasma	incubation in $CaCl_2$ solution after printing	laser-induced forward transfer	mouse NIH-3T3 Swiss albin + human immortalised keratinocyte cell line, HaCaT	$33*10^6$ cells/ml	NA	skin tissue generation	8
ionotropic	sodium alginate	1% w/v	nano-hydroxyapatite + glycerol (10% v/v)		laser-induced forward transfer	EA.hy926 endothelial cell	$30\text{-}50*10^6$ cells/ml	good (non quantitative)	platform	63
ionotropic	sodium alginate (core)	3% w/v	$CaCl_2$ solution (shelf)		co-axial extrusion	rat myocardial cell lines (H9C2)	$1*10^6$ cells/ml	>90% after printing	platform	150
ionotropic	sodium alginate (shelf)	3-5% w/v	$CaCl_2$ solution (core)		coaxial extrusion (self developed)	primary human umbilical vein smooth muscle cells (HUVSMCs)	$10*10^6$ cells/ml	35% after 24h	vascularized tissue engineering	149
ionotropic	sodium alginate of different sizes	1-5 wt%		printing into $CaCl_2$ solution	extrusion	NIH 3T3 fibroblast	$3.5*10^6$ cells/ml	good (non quantitative)	platform	136

self-assembly	collagen (from rat)	0.2wt%	NaOH (neutralization)	droplet ejection	rat smooth muscle cells	0.1-1*10^6 cells/ml	94% after printing		platform	119
self-assembly	collagen (from rat)	1.25-1.75 wt%	NaOH (neutralization)	extrusion	bovine fibrochondrocytes	10*10^6 cells/ml	>90% after printing		cartilage repair	120
self-assembly	collagen (from rat)	86% v/v (no information of original concentration)	NaOH (neutralization)	laser-assisted bioprinting	NIH3T3 fibroblasts and HaCaT keratinocytes	35*10^6 cells/ml	NA	male Balb/c nude mice	skin tissue regeneration	46
self-assembly	collagen type I (from rat tail)	0.24% w/v	polyvinylpyrrolidone (PVP, 0-11.3% w/v) + NaOH (neutralization)	microvalve-based printer	normal human dermal fibroblasts (hDFs)	0.15*10^6 cells/ml	good (non quantitative)		platform	104
self-assembly	dECM	1.5-2.5%		extrusion	NIH3T3 cells	NS	95% after 1 day		platform	76
self-assembly	guanosine + boronic acid + potassium hydroxide (G quadruplex formation)	50 mM, 50 mM and 25 mM		extrusion	adult hDFs	NS	98% after 1 day		platform	133
self-assembly	heart tissue-derived decellularized extracellular matrix (hdECM)	2% w/v	vitamin B2 (0.02% w/v) + vascular endothelial growth factor (VEGF, 10µg/ml)	extrusion	human cardiac progenitor cells (hCPCs) + hMSC	5*10^6 cells/ml	90% after printing	Balb/c nude mice	stem cell patch(cardiac repair) / platform	52
self-assembly	Hydroxypropyl chitin + matrigel	2-3% w/v and 0-30% v/v		extrusion	(hiPSCs	1*10^6 cells/ml	>85% after 3D printing		platform	118
self-assembly	peptides from PeptiGelDesign	original commercial concentration		extrusion	EpH4 (mammary epithelial cells)	4*10^6 cells/ml	good (non quantitative)		platform	132

self-assembly	self-assembling lysine-containing ultrashort Peptides	0.5% w/v		extrusion	hMSC and Caco2 cells	NS	good (non quantitative)	C57BL/6 mice	three-dimensional organotypic cultures	185
self-assembly	silk fibroin	3.75-10% w/v	PEG 400 (40% w/w)	extrusion	hMSC and Mouse NIH/3T3 cells	$2*10^6$ cells/ml	good (non quantitative)	Danforth's short tail (SD) mice	platform	122
thermo-sensitive	block copolymers comprising hydrophilic poly(2-methyl-2-oxazoline) and thermoresponsive poly(2-n-propyl-2-oxazine) (nPrOzi)	20 wt%		extrusion	Murine NIH 3T3 fibroblasts	$1*10^6$ cells/ml	85% after 1 day		platform	126
thermo-sensitive	PU (polyurethane) nanoparticles (PCL et PLA)	25-30%		extrusion	murine neural stem cells	$4*10^6$ cells/ml	40-80% after 24h	zebra fish	central nervous system repair	127

Table 3 Chemical bioinks described in the literature (NA = not assayed, NS = not specified)

GELATION PROCESS	NETWORK PRECURSOR	NETWORK PRECURSOR CONCENTRATION	OTHER COMPONENTS	POST PRINTING PROCESSING	PRINTER TYPE	CELL TYPE	CELLULAR CONCENTRATION	CELLULAR VIABILITY	IN VIVO ASSAYS	APPLICATION	REF.
ENZYMATIC CATALYSE OXIDATION	phenolic hydroxyl (Ph) - alginate + gelatin-Ph	1.5% and 0.5%	horseradish peroxidase (HRP, 50 U/ml)	printing into a H_2O_2 and $CaCl_2$ vat	inkjet (self developed)	SWISS 3T3-albino fibroblasts	$6*10^6$ cells/ml	90% after 24h		platform	181
ENZYMATIC CROSS-LINKING	gelatin + sodium alginate + fibrinogen	10%, 1%, 1% and 1%	transglutaminase (1%)	incubation in $CaCl_2$ solution and thrombin (20U/ml)	extrusion	glioma stem cells, SU3 cells	$0.5*10^6$ cells/ml	85% after printing		brain tumour model	180
ENZYMATIC POLYMERIZATION	thrombin	50 unit/ml	Ca^{2+} (80mM)	printing into a fibrinogen solution (60 mg/ml) and incubation at 37°C after printing	inkjet	hMVEC	$1-8*10^6$ cells/ml	good (non quantitative)		microvasculature fabrication	183
ENZYMATIC REACTION (SCHIFF BASE LINKAGE)	PEG-BA (benzylamine) + glycol chitosan (GC)	7 wt% and 3 wt%	catalase (200U) + Monoamine oxidase B (MAO B, 5 mg/ml)		extrusion	NIH 3T3 cells	NS	>95% after 48h		dynamic platform	182
HYDRAZONE CROSS-LINKING	hyaluronic acid hydrazide + HA-aldehyde	1.5-5 wt% total with equal mass ratio			extrusion	3T3 fibroblasts	$2*10^6$ cells/ml	>80% after 1 day		platform	162
SCHIFF BASE REACTION	gelatin + dextran-aldehyde	5 wt% and 5 wt%		low temperature printing (18°C), 18°C incubation during 2 hours then 37°C	extrusion	hDFs	$1*10^6$ cells/ml	95% after printing		platform	179
THIOL-ACRYLATE REACTION	thiolated HA (CMHA-S) +	2% w/v + 2% w/v	NaOH (neutralization)		extrusion	NIH 3T3 cells	$25*10^6$ cells/ml	good (non quantitative)		synthesis of blood vessel-like structures	177

	four-arm-PEG tetra acrylate									
UV CROSS-LINKING	PEG-DA	10% w/v	Irgacure 2959 (0.05% w/v) + TGF-β3 (10 ng/mL)	UV irradiation after printing	inkjet	hMSCs	$5*10^6$ cells/ml	90% after printing	cartilage tissue engineering	56
UV CROSS-LINKING	acrylated PEG-PCL triblock copolymer	40% w/v	LAP (0.5% w/v)	light irradiation	extrusion	mouse 3T3 fibroblasts	$5*10^6$ cells/ml	90% after 1 day	platform	170
UV CROSS-LINKING	alginate-norbornene modified + PEG dithiol	2 wt% and 10% mol	LAP (2mM)	printing into cell culture medium and UV irradiation after printing	extrusion	mouse L929 fibroblast	$3*10^6$ cells/ml	>90% after printing	platform	106
UV CROSS-LINKING	GelAGE (allyl glycidyl ether)	10-20 wt%	DTT + Ru/SPS (1/10 × 10−3 M)	visible-light irradiation after printing	extrusion	porcine chondrocytes	$3*10^6$ cells/ml	good (non quantitative)	platform	161
UV CROSS-LINKING	Gel-MA	10% w/v	silk fibroin particles (0-1% w/v) + Eosin Y (0.1mM)	PBS washes	digital light processing	NIH 3T3 cells	$1.5*10^6$ cells/ml	>90% after printing	platform	155
UV CROSS-LINKING	Gel-MA	5%	Irgacure 2959 (0.5%) + BMP-2 (20 ng/mL) or TGF-β1 (10 ng/mL) + NaOH (neutralization)	UV irradiation after printing	nanoliter droplets deposition	hMSC	$1*10^6$ cells/ml	>90% after 24h	mimation of the native fibrocartilage phase / platform	55
UV CROSS-LINKING	Gel-MA	10%	Irgacure 2959 (0.05%)	UV irradiation after printing	extrusion	BM-MSCs	$10*10^6$ cells/ml	80% after printing	cartilage tissue engineering	92
UV CROSS-LINKING	Gel-MA	15%	Eosin Y (0.02mM)	PBS washes	stereolithography	NIH 3T3 fibroblasts	$8*10^6$ cells/ml	>80% after 1 day	platform	163

UV CROSS-LINKING	Gel-MA + gellan gum	10% w/v and 1% w/v	PLA micro-carriers functionalized with human recombinant collagen type I loaded with cells (40mg/ml) + Irgacure 2959 (0.1% w/v) + mannose (5.4% w/v)	UV irradiation after printing	extrusion	rat MSCs	$8*10^6$ cells/ml	>70% after 1 day	platform	165
UV CROSS-LINKING	Gel-MA + PEG-DA	0-7.5% and 10-2.5%	Eosin Y (0.01mM)	PBS washes	stereolithography	NIH 3T3 fibroblasts	$5*10^6$ cells/ml	>80% after printing	platform	171
UV CROSS-LINKING	HA-MA + Gel-MA	4% w/v and 6-12% w/v	Irgacure 2959 (0.05% w/v)	UV irradiation after printing	extrusion	hAVICs	$5*10^6$ cells/ml	>90% after printing	bioprinting of heart valve conduit	157
UV CROSS-LINKING	methacrylated silk fibroin	10-30% w/v	LAP (0.2% w/v)	PBS washes	digital light processing	NIH/3T3 fibroblasts	$1\text{-}10*10^6$ cells/ml	>90% after printing	platform	159
UV CROSS-LINKING	PEG-DA	10% w/v	Laponite (4%)	UV irradiation after printing	extrusion	murine preosteoblasts NIH MC3T3 E1-4	$0.01*10^6$ cells/ml	good (non quantitative)	platform	169
UV CROSS-LINKING	PEG-DA	20% w/v	Irgacure 2959 (0.5% w/v) + acryloyl-PEG-RGD (5mM)	PBS washes	stereolithography	NIH/3T3 cells	$1*10^6$ cells/ml	100% after printing	platform	59
UV CROSS-LINKING	PEG-DMA	10% w/v	Irgacure 2959 (0.05% w/v)	UV irradiation after printing	inkjet	human articular chondrocytes	$8*10^6$ cells/ml	85% after printing	cartilage repair	168

Table 4 Complex bioinks described in the literature (NA = not assayed, NS = not specified)

TYPE OF STRUCTURE	GELATION PROCESS	NETWORK PRECURSOR	NETWORK PRECURSOR CONCENTRATION	OTHER COMPONENTS	POST PRINTING PROCESSING	PRINTER TYPE	CELL TYPE	CELLULAR CONCENTRATION	CELLULAR VIABILITY	IN VIVO ASSAYS	APPLICATION	REF.
COMPLEX (2 STEPS CROSS-LINKING)	aggregation and chemical cross-linking	thiolated gelatin + amphiphilic peptides	2.25 wt% and 0.75 wt%		soaking in a dimaleimide-PEG (5%) and $CaCl_2$ (25 mM) vat	extrusion	SV40 immortalized mouse cholangiocytes (SV40SM)	$0.2*10^6$ cells/ml	good (non quantitative)		bile duct repair	178
COMPLEX (2 STEPS CROSS-LINKING)	UV cross-linking and aggregation	Gel-MA + gelatin	5-30% w/v and 8-10% w/v	LAP (0.5% w/v)	cold receiving plate during printing and UV irradiation during and after	extrusion	BM-MSCs	$5*10^6$ cells/ml	90% after printing		platform	156
COMPLEX (BIOINK WITH MICROSPHERES)	self-assembly	agarose + collagen	1.5% w/v and 1.5 mg/ml	cell-seeded poly(D,L-lactic-co-glycolic acid) (PLGA) porous microspheres (20% v/v) + NaOH (neutralization)	printing is done on iced platform then incubation at 37°C	extrusion (multipipet)	fibroblasts L929 and Rat2, myoblasts C2C12 and A10, and the epithelial TR146 cells	$83*10^6$ cells/g of microspheres	>90% after printing		platform	100
COMPLEX (BIOINK WITH NP)	UV cross-linking	PEG-DMA	20% w/v	bioactive glass nanoparticles (BG 45S5, 1-2% w/v) + hydroxyapatite (1-2% w/v) + Irgacure 2959 (0.05%)	UV irradiation during printing	inkjet (modified)	hBM-MSCs	$6*10^6$ cells/ml	70% after 24h		bone tissue engineering	101

COMPLEX (BIOINK WITH PLASTIC FIBERS)	ionotropic gelation	sodium alginate	2.5-3.5 wt%	PLA sub-micron fibers (2%)	$CaCl_2$ solution (0.2M) spraying during printing	extrusion	human articular chondrocytes	$3*10^6$ cells/ml	>80% after printing		cartilage regeneration	[148]
COMPLEX (DECORATED BIOINK)	UV cross-linking	PEG-DMA	10% w/v	acrylated GRGDS (1mM) + acrylated MMP-sensitive peptides (1mM) + I-2959 (0.05% w/v)	UV irradiation after printing	inkjet	hBM-MSCs	$6*10^6$ cells/ml	90% after 24h		platform	[57]
COMPLEX (DECORATED BIOINK)	UV cross-linking	PEG-DMA	10% w/v	acrylated GRGDS (1mM) + acrylated MMP-sensitive peptides (1mM) + I-2959 (0.05% w/v)	UV irradiation after printing	inkjet	hBM-MSCs	$6*10^6$ cells/ml	NA	C57BL/6 J mice	cartilage repair	[58]
COMPLEX (MULTICOMPONENT BIOINK WITH NP)	UV cross-linking and ionotropic gelation	Gel-MA + kappa carrageenan	10% w/v and 1% w/v	2D nanosilicates (2% w/v) + Irgacure 2959 (0.25% w/v)	UV irradiation after printing and incubation in KCl solution	extrusion	hMSCs	$0.333*10^6$ cells/ml	90% after printing		platform	[102]
COMPOSITE (1 PLASTIC SUPPORT + 1 BIOINK + 1 CELL SUSPENSION)	ionotropic gelation and aggregation	1. polydopamine-calcium silicate PCL 2. sodium alginate + gelatin 3. culture medium	2. 5% and 30%			extrusion for 1. and 2., inkjet for 3.	HUVEC in 2. + Wharton's jelly mesenchymal stem cells (WJMSC) in 3.	$10*10^6$ cells/ml in 2., NS in 3.	good (non quantitative)		bone tissue engineering	[114]
COMPOSITE (1 PLASTIC SUPPORT + 1 BIOINK)	enzymatic cross-linking	1. PCL and pluronic F127 2. fibrinogen + collagen (from rat) 3. thrombin	1. 10% w/v and 5% w/v in acetone 2. 10 mg/ml and 1.5			electrospinning (1.) and inkjet (self developed, 2. and 3.)	rabbit chondrocytes	$3-4*10^6$ cells/ml in 2.	81% after 1 week	nu/nu mice	cartilage repair	[94]

			mg/ml 3. 20 UI/ml									
COMPOSITE (1 PLASTIC SUPPORT + 1 BIOINK)	ionotropic gelation	1. PCL 2. sodium alginate + RGD-alginate	2. 1% total	nano hydroxyapatite pDNA complexes	incubation in $CaCl_2$ solution	extrusion	MSCs	$10*10^6$ cells/ml in 2.	70% after 1 day		bone tissue engineering	60
COMPOSITE (1 PLASTIC SUPPORT + 1 BIOINK)	ionotropic gelation	1. PCL 2. sodium alginate	2. 4-6%	TGF-β (10 ng/mL)	incubation in $CaCl_2$ and NaCl solution	extrusion	human primary nasal septal cartilage chondrocyte	$1*10^6$ cells/ml in 2.	85% after printing	female nude mice	cartilage repair	53
COMPOSITE (1 PLASTIC SUPPORT + 1 BIOINK)	ionotropic gelation	1. pluronic 2. gellan gum + sodium alginate	1. 30% 2. 3% and 2%	1. sodium chloride (150 mM) + strontium chloride (20 mM) 2. hydroxyapatite or BioCartilage product (40% w/w polymer)	incubation in $SrCl_2$ solution	extrusion	bovine chondrocytes	$6*10^6$ cells/ml in 2.	80% after printing		cartilage repair / construct	64
COMPOSITE (1 PLASTIC SUPPORT + 1 BIOINK)	ionotropic gelation	1. PCL 2. sodium alginate	2. 4% w/v		incubation in $CaCl_2$ solution	extrusion	primary rabbit chondrocytes	$3*10^6$ cells/ml in 2.	good (non quantitative)	New Zealand white rabbits	auricular cartilage repair	96
COMPOSITE (1 PLASTIC SUPPORT + 1 BIOINK)	ionotropic gelation and self-assembly	1. PCL 2. CELLINK® (nanofibrilated cellulose + sodium alginate)	2. 2% w/v and 0.5% w/v		incubation in $CaCl_2$ solution	extrusion (1.) and inkjet (2.)	human nasal chondrocytes	$20*10^6$ cells/ml in 2.	70% after printing		auricular cartilage regeneration	93
COMPOSITE (1 PLASTIC SUPPORT + 1 BIOINK)	self-assembly	1. PCL 2. Matrigel™	1. 1.25-1.66 g/ml in chloroform 2. 9 mg/ml	1. 13-93B3 borate glass (10-50 wt%)		extrusion	human adipose stem cells (ASCs)	$10*10^6$ cells/ml in 2.	70% after 24h		bone tissue engineering	113

COMPOSITE (1 PLASTIC SUPPORT + 1 BIOINK)	self-assembly	1. PCL 2. dECM (from adipose, cartilage or heart)	2. 3%	2. NaOH (neutralization)		extrusion (self developed)	hASCs, hTMSCs or Rat myoblast cells (L6, ATCC CRL-1458)	1-5*10^6 cells/ml in 2.	95% after 24h		tissue reconstruction / platform	77
COMPOSITE (1 PLASTIC SUPPORT + 1 BIOINK)	self-assembly	1. PCL 2. decellularized adipose tissue	2. NS	2. NaOH (neutralization)		extrusion (self developed)	hASCs	2-5*10^6 cells/ml in 2.	93% after 24h	nude mice	soft tissue regeneration	5
COMPOSITE (1 PLASTIC SUPPORT + 1 BIOINK)	UV cross-linking	1) PCL 2) HA-SH + poly(allyl glycidyl ether-co-glycidyl) + HA	2. 5 wt%, 5 wt% and 1 wt%	2. I-2959 (0.05 wt%) + NaOH (neutralization)	UV irradiation after printing	extrusion	hBM-MSCs	6*10^6 cells/ml in 2.	good (non quantitative)		cartilage engineering	97
COMPOSITE (1 PLASTIC SUPPORT + 1 HYDROGEL + 2 BIOINKS)	self-assembly	1. PCL 2. atelocollagen 3. Cucurbit[6]uril -hyaluronic acid 4. 1,6-diaminohexane-hyaluronic acid	2. 3% w/v 3. 5% w/v 4. 5% w/v	2. BMP-2 (5µg/ml) 3. TGF-β (0.1µg/ml)		extrusion (self developed)	human turbinate-derived mesenchymal stromal cells (hTMSCs)	1*10^6 cells/ml in 2. and 2*10^6 cells/ml in3.	good (non quantitative)	rabbits	osteochondral tissue regeneration	54
COMPOSITE (1 PLASTIC SUPPORT + 1 SACRIFICIAL INK + 3 BIOINKS)	UV cross-linking	1. poly(dimethyl siloxane) (PDMS) 2. Pluronic F127 (fugitive) 3. Gel-MA 4. Gel-MA 5. Gel-MA	2. 40 wt% in water 3. 15% w/v 4. 15% w/v 5. 15% w/v	3. Irgacure 2959 (0.3 wt%) 4. Irgacure 2959 (0.3 wt%) 5. Irgacure 2959 (0.3 wt%)	UV irradiation after printing and incubation at 4°C to remove the fugitive ink	extrusion	C3H/10T1/2, Clone 8 cells (ATCC CCL-226TM, in 4.) and GFP-expressing human neonatal dermal fibroblast cells (in 5.)	2*10^6 cells/ml in 4. and 5.	60-70% after printing		vascularized tissue engineering	98

COMPOSITE (1 PLASTIC SUPPORT + 2 BIOINKS)	aggregation and enzymatic cross-linking	1. poly (e-caprolactone) (PCL) and Poly(lactide-co-caprolactone) (PLCL) 2. gelatin + fibrinogen + HA 3. gelatin + fibrinogen + HA	2. 35 mg/ml, 30 mg/ml and 3 mg/ml 3. 35 mg/ml, 30 mg/ml and 3 mg/ml		incubation in thrombin solution	extrusion	urothelial cells (UCs, in 2.) and smooth muscle cells (SMCs, in 3.)	$10*10^6$ cells/ml in 2. and 3.	90% after 1 day		urethra production	82
COMPOSITE (1 PLASTIC SUPPORT + 2 BIOINKS)	ionotropic gelation	1. PCL 2. sodium alginate 3. sodium alginate	2. 4% w/v 3. 4% w/v		incubation in $CaCl_2$ and NaCl solution	extrusion	human nasal septum cartilage chondrocytes (in 2.) and MG63 human osteoblast cells (in 3.)	$1*10^6$ cells/ml in 2. and 3.	90-95% after 24h		osteochondral tissue regeneration	95
COMPOSITE (1 PLASTIC SUPPORT + 3 BIOINKS)	self-assembly	1. PCL 2. heart tissue-derived decellularized extracellular matrix (HdECM) 3. HdECM 4. HdECM	2. 20 mg/ml 3. 20 mg/ml 4. 20 mg/ml	2. NaOH (neutralization) + vitamin B2 (0.02% w/v) 3. NaOH + vitamin B2 (0.02% w/v) + VEGF (10 µg/ml) 4. NaOH + vitamin B2 (0.02% w/v) + VEGF (10 µg/ml)	UV irradiation after printing and incubation at 37°C	extrusion	human cardiac progenitor cells (hCPCs, in 2. and 4.) and MSCs (in 3. and 4.)	$5*10^6$ cells/ml in 2., 3. and 4.	> 90% after printing	Balb/c nude mice	cardiac repair	52
HETEROGENEOUS (1 BIOINK + 1 HYDROGEL WITH CROSS-LINKER)	UV cross-linking	1. Gel-Ma + HA-MA (core) 2. Gel-Ma + HA-MA (shell)	1. 10 wt% and 2 wt% 2. 10 wt% and 2 wt%	2. VA-086 (0.5 wt%)	light irradiation after printing	co-axial extrusion (biopen self developed)	sheep MSC in 1.	$2.5*10^6$ cells/ml in 1.	97% after printing	Sheep	cartilage repair	164

HETEROGENEOUS (1 BIOINK + 1 SOLUTION OF CROSS-LINKER)	ionotropic gelation and UV cross-linking	1. sodium alginate + GelMA + PEGTA (shelf) 2. CaCl2 (core)	1. 1-3%, 5-7% and 1-3% 2. 0.3M	1. Irgacure 2959 (0.25% w/v)	UV irradiation after printing and EDTA solution washed to remove alginate	coaxial extrusion	HUVECs hMSCs	$3*10^6$ cells/ml in 1.	80% after printing		vascularized tissue engineering	[167]
HETEROGENEOUS (1 BIOINK + 2 SOLUTIONS OF CROSS-LINKER)	ionotropic gelation	1. sodium alginate (core) 2. CaCl2 (inside shelf) 3. CaSo4 (outside shelf)	1. 3.2%			coaxial extrusion	MDA-MB-231 human adenocarcinoma cells (in 1.) and RAW 264.7 mouse macrophage cells (in 2.)	$5*10^6$ cells/ml in 1. and $4.5*10^6$ cells/ml in 2.	90% after 24h		tumour microenvironment model	[151]
HETEROGENEOUS (1 BIOINK + 1 SOLUTION OF CROSS-LINKER)	self-assembly and enzymatic cross-linking	1. fibrinogen + collagen 2. thrombin	1. 25 mg/ml and 1.1 mg/ml 2. 20 IU/ml			extrusion (self developed)	human amniotic fluid-derived stem cells (hAFS) or hBMSCs	$16.6*10^6$ cells/ml in 1.	NA	nu/nu mice	wound repair	[117]
HETEROGENEOUS (1 BIOINK + 1 SOLUTION OF CROSS-LINKER)	chemical cross-linking and ionotropic gelation	1. sodium alginate + gelatin (core) 2. $CaCl_2$ (shelf)	1. 2% w/v and 10% w/v 2. 0.3 M		Incubation in genipin solution (0.01% w/v) after printing	coaxial extrusion	hMSCs	NS	>90% after printing		platform	[186]
HETEROGENEOUS (1 BIOINK + 1 HYDROGEL)	aggregation and UV cross-linking	1. gelatin 2. PEG-DMA covering (no printing)	1. 3% w/v 2. 20% w/v	2. 2-hydroxy-2-methylpropiophenone (0.1% w/v)	UV irradiation after covering	droplet ejection (self developed)	MCF-7 human breast cancer cells	$0.5\text{-}1*10^6$ cells/ml in 1.	100% after 1h		cellular spheroids fabrication	[187]
HETEROGENEOUS (1 BIOINK + 1 HYDROGEL)	UV cross-linking and ionotropic gelation	1. Gel-MA (core) 2. sodium alginate (sheath)	1. 1-2% 2. 1%	1. $CaCl_2$ (1%) and PI (0.2%)	UV irradiation after printing	co-axial extrusion	HUVECs, MDA-MB-231, MCF7 breast cancer cells, or NIH/3T3 mouse fibroblasts	$2*10^6$ cells/ml in 1.	>45% after printing		Micro-fiber construct	[166]

HETEROGENEOUS (1 BIOINK + 1 SOLUTION OF CROSS-LINKER)	ionotropic gelation and UV cross-linking	1. sodium alginate + Gel-MA (core) 2. $CaCl_2$ (shelf)	1. 2% w/v and 7% w/v 2. 0.3 M	NS cross-linker	UV irradiation after printing	coaxial extrusion	HepG2/C3A hepatocytes	NS	>90% after printing		platform	186
HETEROGENEOUS (1 BIOINK + 1 SOLUTION OF CROSS-LINKER)	self-assembly and ionotropic gelation	1. sodium alginate + collagen (core) 2. $CaCl_2$ (shelf)	1. 2% w/v and 1 mg/ml 2. 0.3 M	1. NaOH (neutralization)		coaxial extrusion	hMSCs, and MDA-MB-231 breast cancer cells	NS	>90% after printing		platform	186
HETEROGENEOUS (1 HYDROGEL + 1 BIOINK)	self-assembly	1. polypeptide–DNA conjugate (poly(l-glutamic acid240-co-g-propargyl-l-glutamate20) 2. double-stranded DNA	1. 6 wt% 2. 2mM			inkjet	AtT-20 cells (an anterior pituitary cell line	$1.6*10^6$ cells/ml in 1.	99% after printing		platform	115
HETEROGENEOUS (1 SACRIFICIAL INK + 2 BIOINKS)	UV cross-linking	1. pluronic (sacrificial) 2. Gel-MA 3. Gel-MA	1. 40% w/v 2. 10% w/v 3. 10% w/v	2. Irgacure 2959 (0.1% w/v) 3. Irgacure 2959 (0.1% w/v)	UV irradiation after printing	extrusion	MSC in 2. and ACPC in 3.	$20*10^6$ cells/ml in 2. and 3.	> 75% after 1 day		cartilage repair	10
HETEROGENEOUS (1 SACRIFICIAL INK WITH CROSS-LINKER + 1 BIOINK)	aggregation and enzymatic cross-linking	1. Pluronic F127 2. gelatin + fibrinogen	1. 38 wt% 2. 7.5% w/v and 10 mg/ml	1. thrombin (100 U/ml) 2. transglutaminase (0.1 wt%)	Stored at 37°c for 1h after printing then cooling at 4°C to remove the sacrificial ink	extrusion	hMSCs	NS	>60% after printing		vascularized tissue engineering	91
HETEROGENEOUS (2 BIOINKS)	UV cross-linking	1. Gel-MA 2. PEG-DA	1. 5% w/v 2. 5% w/v 1/4-4/1 of 1. and 2.	1. TCI 0.5% w/v 2. TCI 0.5% w/v	UV irradiation after printing	extrusion	Periodontal ligament stem cells (PDLSCs)	$1*10^6$ cells/ml in 1. and 2.	> 80% after printing	rats	*in vivo* repair of alveolar bone defect	172

HETEROGENEOUS AND COMPLEX (BIOINK WITH NANORODS + CROSS-LINKER SOLUTION)	ionotropic gelation and UV cross-linking	1. sodium alginate + Gel-MA + gold nanorod (GNR)-Gel-MA (core) 2. $CaCl_2$ solution (shelf)	1. 2% w/v, 7% w/v and 0-0.5 mg/ml	1. Irgacure 2959 (0.25 %)	UV irradiation after printing	coaxial extrusion	cardiac fibroblasts	$5*10^6$ cells/ml in 1.	80% after printing		cardiac repair	99
HETEROGENEOUS AND COMPLEX (BIOINK WITH SPHEROIDS + CROSS-LINKER SOLUTION)	ionotropic gelation	1. sodium alginate (core) 2. $CaCl_2$ solution (shelf) 3. sodium alginate spheroids (2^{nd} extruder)	1. 4% w/v 3. 4% w/v			coaxial extrusion (self developed)	Cartilage progenitor cells (CPCs)	$4*10^6$ cells/ml in 3.	60% after 24h		tissue engineering	103
HETEROGENEOUS AND COMPLEX (TUBULAR BIOINK CONSTRUCT WITH MICROSPHERES)	ionotropic gelation and self-assembly	1. vascular dECM + sodium alginate (shelf) 2. pluronic F-127 (fugitive, core)	1. 3% and 2 wt% 2. 40 wt%	1. Atorvastatin-loaded PLGA microspheres (15 mg/ml) + NaOH (neutralization) 2. $CaCl_2$	incubation in cell media at 37°C (removal of fugitive ink and cross-linking)	coaxial extrusion (self developed)	mouse endothelial progenitor cells	$10*10^6$ cells/ml in 1.	80% after printing	male eight-week-old Balb/c nude mice	blood vessel construction	65
HETEROGENEOUS (1 HYDROGEL + 1 SOLUTION OF CROSS-LINKER AND CELLS)	ionotropic gelation	1. alginate + methycellulose 2. trisodium citrate	1. 3 wt% and 9 wt% 2. 15 mg/ml	1. $CaCl_2$		extrusion	mouse fibroblasts L929	$3*10^6$ cells/ml in 2.	90% after printing		platform	116

Conflicts of interest

The authors have declared that no conflict of interest exists.

Acknowledgments

This work was funded by the ANR (Agence Nationale de la Recherche), the French National Research Agency (ANR-16-CE18-0003).

Notes and references

1 D. Richards, J. Jia, M. Yost, R. Markwald and Y. Mei, *Ann. Biomed. Eng.*, 2017, **45**, 132–147.
2 I. Cicha, R. Detsch, R. Singh, S. Reakasame, C. Alexiou and A. R. Boccaccini, *Curr. Opin. Biomed. Eng.*, 2017, **2**, 83–89.
3 E. Hoch, G. E. M. Tovar and K. Borchers, *Eur. J. Cardiothorac. Surg.*, 2014, **46**, 767–778.
4 C. Mandrycky, Z. Wang, K. Kim and D.-H. Kim, *Biotechnol. Adv.*, 2016, **34**, 422–434.
5 F. Pati, D.-H. Ha, J. Jang, H. H. Han, J.-W. Rhie and D.-W. Cho, *Biomaterials*, 2015, **62**, 164–175.
6 A. Blaeser, D. F. Duarte Campos and H. Fischer, *Curr. Opin. Biomed. Eng.*, , DOI:10.1016/j.cobme.2017.04.003.
7 T. Boland, X. Tao, B. J. Damon, B. Manley, P. Kesari, S. Jalota and S. Bhaduri, *Mater. Sci. Eng. C*, 2007, **27**, 372–376.
8 L. Koch, A. Deiwick, S. Schlie, S. Michael, M. Gruene, V. Coger, D. Zychlinski, A. Schambach, K. Reimers, P. M. Vogt and B. Chichkov, *Biotechnol. Bioeng.*, 2012, **109**, 1855–1863.
9 S. P. Tarassoli, Z. M. Jessop, A. Al-Sabah, N. Gao, S. Whitaker, S. Doak and I. S. Whitaker, *J. Plast. Reconstr. Aesthet. Surg.*, , DOI:10.1016/j.bjps.2017.12.006.
10 R. Levato, W. R. Webb, I. A. Otto, A. Mensinga, Y. Zhang, M. van Rijen, R. van Weeren, I. M. Khan and J. Malda, *Acta Biomater.*, 2017, **61**, 41–53.
11 T. Guo, J. Lembong, L. G. Zhang and J. P. Fisher, *Tissue Eng. Part B Rev.*, 2017, **23**, 225–236.
12 G. O'Connell, J. M. Garcia and A. A. Jamali, *ACS Biomater. Sci. Eng.*, , DOI:10.1021/acsbiomaterials.6b00587.
13 S. Adepu, N. Dhiman, A. Laha, C. S. Sharma, S. Ramakrishna and M. Khandelwal, *Curr. Opin. Biomed. Eng.*, 2017, **2**, 22–28.
14 N. E. Fedorovich, J. Alblas, W. E. Hennink, F. C. Öner and W. J. A. Dhert, *Trends Biotechnol.*, 2011, **29**, 601–606.
15 X. Du, B. Yu, P. Pei, H. Ding, B. Yu and Y. Zhu, *J. Mater. Chem. B*, 2018, **6**, 499–509.
16 H. Ma, J. Chang and C. Wu, in *Developments and Applications of Calcium Phosphate Bone Cements*, eds. C. Liu and H. He, Springer Singapore, Singapore, 2018, vol. 9, pp. 497–516.
17 S. Ji and M. Guvendiren, *Front. Bioeng. Biotechnol.*, , DOI:10.3389/fbioe.2017.00023.
18 D. Kilian, T. Ahlfeld, A. R. Akkineni, A. Lode and M. Gelinsky, *MRS Bull.*, 2017, **42**, 585–592.
19 T. A. Mir and M. Nakamura, *Tissue Eng. Part B Rev.*, 2017, **23**, 245–256.
20 S. V. Murphy and A. Atala, *Nat. Biotechnol.*, 2014, **32**, 773–785.
21 S. Vijayavenkataraman, W.-C. Yan, W. F. Lu, C.-H. Wang and J. Y. H. Fuh, *Adv. Drug Deliv. Rev.*, , DOI:10.1016/j.addr.2018.07.004.
22 W. Peng, D. Unutmaz and I. T. Ozbolat, *Trends Biotechnol.*, 2016, **34**, 722–732.
23 H. Zhao, F. Yang, J. Fu, Q. Gao, A. Liu, M. Sun and Y. He, *ACS Biomater. Sci. Eng.*, 2017, **3**, 3083–3097.
24 P. Zhuang, A. X. Sun, J. An, C. K. Chua and S. Y. Chew, *Biomaterials*, 2018, **154**, 113–133.
25 J. Vanderburgh, J. A. Sterling and S. A. Guelcher, *Ann. Biomed. Eng.*, 2017, **45**, 164–179.
26 A. Memic, A. Navaei, B. Mirani, J. A. V. Cordova, M. Aldhahri, A. Dolatshahi-Pirouz, M. Akbari and M. Nikkhah, *Biotechnol. Lett.*, 2017, **39**, 1279–1290.
27 T. Q. Huang, X. Qu, J. Liu and S. Chen, *Biomed. Microdevices*, 2014, **16**, 127–132.
28 S. Samavedi and N. Joy, *Curr. Opin. Biomed. Eng.*, 2017, **2**, 35–42.
29 V. Mourino and A. R. Boccaccini, *J. R. Soc. Interface*, 2010, **7**, 209–227.
30 J. Y. Park, G. Gao, J. Jang and D.-W. Cho, *J Mater Chem B*, 2016, **4**, 7521–7539.
31 I. T. Ozbolat, W. Peng and V. Ozbolat, *Drug Discov. Today*, 2016, **21**, 1257–1271.
32 I. T. Ozbolat, K. K. Moncal and H. Gudapati, *Addit. Manuf.*, 2017, **13**, 179–200.

33 Ian Freshney, in *Culture of Animal Cells: A Manual of Basic Technique and Specialized Applications*, John Wiley & Sons, 2015.
34 K. Nair, M. Gandhi, S. Khalil, K. C. Yan, M. Marcolongo, K. Barbee and W. Sun, *Biotechnol. J.*, 2009, **4**, 1168–1177.
35 Y.-J. Seol, H.-W. Kang, S. J. Lee, A. Atala and J. J. Yoo, *Eur. J. Cardiothorac. Surg.*, 2014, **46**, 342–348.
36 S. Kyle, Z. M. Jessop, A. Al-Sabah and I. S. Whitaker, *Adv. Healthc. Mater.*, 2017, 1700264.
37 I. T. Ozbolat and M. Hospodiuk, *Biomaterials*, 2016, **76**, 321–343.
38 H. Gudapati, M. Dey and I. Ozbolat, *Biomaterials*, 2016, **102**, 20–42.
39 B. R. Ringeisen, C. M. Othon, J. A. Barron, D. Young and B. J. Spargo, *Biotechnol. J.*, 2006, **1**, 930–948.
40 M. Duocastella, M. Colina, J. M. Fernández-Pradas, P. Serra and J. L. Morenza, *Appl. Surf. Sci.*, 2007, **253**, 7855–7859.
41 B. Guillotin, S. Catros and F. Guillemot, in *Laser Technology in Biomimetics*, eds. V. Schmidt and M. R. Belegratis, Springer Berlin Heidelberg, Berlin, Heidelberg, 2013, pp. 193–209.
42 C. Mézel, A. Souquet, L. Hallo and F. Guillemot, *Biofabrication*, 2010, **2**, 014103.
43 N. R. Schiele, D. T. Corr, Y. Huang, N. A. Raof, Y. Xie and D. B. Chrisey, *Biofabrication*, 2010, **2**, 032001.
44 D. J. Odde and M. J. Renn, *Biotechnol. Bioeng.*, 2000, **67**, 312–318.
45 C. M. B. Ho, A. Mishra, K. Hu, J. An, Y.-J. Kim and Y.-J. Yoon, *ACS Biomater. Sci. Eng.*, 2017, **3**, 2198–2214.
46 S. Michael, H. Sorg, C.-T. Peck, L. Koch, A. Deiwick, B. Chichkov, P. M. Vogt and K. Reimers, *PLoS ONE*, 2013, **8**, e57741.
47 R. J. Mondschein, A. Kanitkar, C. B. Williams, S. S. Verbridge and T. E. Long, *Biomaterials*, 2017, **140**, 170–188.
48 I. Donderwinkel, J. C. M. van Hest and N. R. Cameron, *Polym Chem*, , DOI:10.1039/C7PY00826K.
49 M. Hospodiuk, M. Dey, D. Sosnoski and I. T. Ozbolat, *Biotechnol. Adv.*, 2017, **35**, 217–239.
50 R. R. Jose, M. J. Rodriguez, T. A. Dixon, F. Omenetto and D. L. Kaplan, *ACS Biomater. Sci. Eng.*, 2016, **2**, 1662–1678.
51 B. C. Gross, J. L. Erkal, S. Y. Lockwood, C. Chen and D. M. Spence, *Anal. Chem.*, 2014, **86**, 3240–3253.
52 J. Jang, H.-J. Park, S.-W. Kim, H. Kim, J. Y. Park, S. J. Na, H. J. Kim, M. N. Park, S. H. Choi, S. H. Park, S. W. Kim, S.-M. Kwon, P.-J. Kim and D.-W. Cho, *Biomaterials*, 2017, **112**, 264–274.
53 J. Kundu, J.-H. Shim, J. Jang, S.-W. Kim and D.-W. Cho, *J. Tissue Eng. Regen. Med.*, 2015, **9**, 1286–1297.
54 J.-H. Shim, K.-M. Jang, S. K. Hahn, J. Y. Park, H. Jung, K. Oh, K. M. Park, J. Yeom, S. H. Park, S. W. Kim, J. H. Wang, K. Kim and D.-W. Cho, *Biofabrication*, 2016, **8**, 014102.
55 U. A. Gurkan, R. El Assal, S. E. Yildiz, Y. Sung, A. J. Trachtenberg, W. P. Kuo and U. Demirci, *Mol. Pharm.*, 2014, **11**, 2151–2159.
56 G. Gao, K. Hubbell, A. F. Schilling, G. Dai and X. Cui, in *3D Cell Culture*, ed. Z. Koledova, Springer New York, New York, NY, 2017, vol. 1612, pp. 391–398.
57 G. Gao, T. Yonezawa, K. Hubbell, G. Dai and X. Cui, *Biotechnol. J.*, 2015, **10**, 1568–1577.
58 G. Gao, X.-F. Zhang, K. Hubbell and X. Cui, *Biotechnol. Bioeng.*, 2017, **114**, 208–216.
59 V. Chan, P. Zorlutuna, J. H. Jeong, H. Kong and R. Bashir, *Lab. Chip*, 2010, **10**, 2062.
60 G. M. Cunniffe, T. Gonzalez-Fernandez, A. Daly, B. N. Sathy, O. Jeon, E. Alsberg and D. J. Kelly, *Tissue Eng. Part A*, , DOI:10.1089/ten.tea.2016.0498.
61 S. T. Bendtsen, S. P. Quinnell and M. Wei, *J. Biomed. Mater. Res. A*, 2017, **105**, 1457–1468.
62 S. T. Bendtsen and M. Wei, *J. Biomed. Mater. Res. A*, 2017, **105**, 3262–3272.
63 F. Guillemot, A. Souquet, S. Catros, B. Guillotin, J. Lopez, M. Faucon, B. Pippenger, R. Bareille, M. Rémy, S. Bellance, P. Chabassier, J. C. Fricain and J. Amédée, *Acta Biomater.*, 2010, **6**, 2494–2500.
64 M. Kesti, C. Eberhardt, G. Pagliccia, D. Kenkel, D. Grande, A. Boss and M. Zenobi-Wong, *Adv. Funct. Mater.*, 2015, **25**, 7406–7417.
65 G. Gao, J. H. Lee, J. Jang, D. H. Lee, J.-S. Kong, B. S. Kim, Y.-J. Choi, W. B. Jang, Y. J. Hong, S.-M. Kwon and D.-W. Cho, *Adv. Funct. Mater.*, 2017, 1700798.
66 M. Djabourov, J.-P. Lechaire and F. Gaill, *Biorheology*, 1993, **30**, 191–205.
67 D. H. Hogg and B. Blomback, *Thromb. Res.*, 1978, **12**, 953–964.
68 S. Chawla, S. Midha, A. Sharma and S. Ghosh, *Adv. Healthc. Mater.*, 2018, 1701204.
69 E. Axpe and M. Oyen, *Int. J. Mol. Sci.*, 2016, **17**, 1976.
70 I. B. Bajaj, S. A. Survase, P. S. Saudagar and R. S. Singhal, 2007, 14.
71 J. T. Oliveira, L. Martins, R. Picciochi, P. B. Malafaya, R. A. Sousa, N. M. Neves, J. F. Mano and R. L. Reis, *J. Biomed. Mater. Res. A*, 2009, **9999A**, NA-NA.
72 J. A. Burdick and G. D. Prestwich, *Adv. Mater.*, 2011, **23**, H41–H56.

73 J. Necas, L. Bartosikova, P. Brauner and J. Kolar, *Veterinární Medicína*, 2008, **53**, 397–411.
74 C. C. Piras, S. Fernández-Prieto and W. M. De Borggraeve, *Biomater. Sci.*, 2017, **5**, 1988–1992.
75 C. T. Buckley, S. D. Thorpe, F. J. O'Brien, A. J. Robinson and D. J. Kelly, *J. Mech. Behav. Biomed. Mater.*, 2009, **2**, 512–521.
76 G. Ahn, K.-H. Min, C. Kim, J.-S. Lee, D. Kang, J.-Y. Won, D.-W. Cho, J.-Y. Kim, S. Jin, W.-S. Yun and J.-H. Shim, *Sci. Rep.*, , DOI:10.1038/s41598-017-09201-5.
77 F. Pati, J. Jang, D.-H. Ha, S. Won Kim, J.-W. Rhie, J.-H. Shim, D.-H. Kim and D.-W. Cho, *Nat. Commun.*, , DOI:10.1038/ncomms4935.
78 M. He and A. Callanan, *Tissue Eng. Part B Rev.*, 2013, **19**, 194–208.
79 J. M. Jang, S.-H.-T. Tran, S. C. Na and N. L. Jeon, *ACS Appl. Mater. Interfaces*, 2015, **7**, 2183–2188.
80 G. Benton, I. Arnaoutova, J. George, H. K. Kleinman and J. Koblinski, *Adv. Drug Deliv. Rev.*, 2014, **79**–**80**, 3–18.
81 C.-C. Lin and K. S. Anseth, *Pharm. Res.*, 2009, **26**, 631–643.
82 K. Zhang, Q. Fu, J. Yoo, X. Chen, P. Chandra, X. Mo, L. Song, A. Atala and W. Zhao, *Acta Biomater.*, 2017, **50**, 154–164.
83 M. S. Lopes, A. L. Jardini and R. M. Filho, *Procedia Eng.*, 2012, **42**, 1402–1413.
84 L. Tan, X. Yu, P. Wan and K. Yang, *J. Mater. Sci. Technol.*, 2013, **29**, 503–513.
85 M. Abedalwafa, F. Wang, L. Wang and C. Li, 18.
86 T. Patrício, M. Domingos, A. Gloria and P. Bártolo, *Procedia CIRP*, 2013, **5**, 110–114.
87 S. Farah, D. G. Anderson and R. Langer, *Adv. Drug Deliv. Rev.*, 2016, **107**, 367–392.
88 B. Zhang, B. Seong, V. Nguyen and D. Byun, *J. Micromechanics Microengineering*, 2016, **26**, 025015.
89 G. Dumortier, J. L. Grossiord, F. Agnely and J. C. Chaumeil, *Pharm. Res.*, 2006, **23**, 2709–2728.
90 M. Bohorquez, C. Koch, T. Trygstad and N. Pandit, *J. Colloid Interface Sci.*, 1999, **216**, 34–40.
91 D. B. Kolesky, K. A. Homan, M. A. Skylar-Scott and J. A. Lewis, *Proc. Natl. Acad. Sci.*, 2016, **113**, 3179–3184.
92 A. C. Daly, S. E. Critchley, E. M. Rencsok and D. J. Kelly, *Biofabrication*, 2016, **8**, 045002.
93 H. Martínez Ávila, S. Schwarz, N. Rotter and P. Gatenholm, *Bioprinting*, 2016, **1**–**2**, 22–35.
94 T. Xu, K. W. Binder, M. Z. Albanna, D. Dice, W. Zhao, J. J. Yoo and A. Atala, *Biofabrication*, 2012, **5**, 015001.
95 J.-H. Shim, J.-S. Lee, J. Y. Kim and D.-W. Cho, *J. Micromechanics Microengineering*, 2012, **22**, 085014.
96 J. Y. Park, Y.-J. Choi, J.-H. Shim, J. H. Park and D.-W. Cho, *J. Biomed. Mater. Res. B Appl. Biomater.*, 2017, **105**, 1016–1028.
97 S. Stichler, T. Böck, N. Paxton, S. Bertlein, R. Levato, V. Schill, W. Smolan, J. Malda, J. Teßmar, T. Blunk and J. Groll, *Biofabrication*, 2017, **9**, 044108.
98 D. B. Kolesky, R. L. Truby, A. S. Gladman, T. A. Busbee, K. A. Homan and J. A. Lewis, *Adv. Mater.*, 2014, **26**, 3124–3130.
99 K. Zhu, S. R. Shin, T. van Kempen, Y.-C. Li, V. Ponraj, A. Nasajpour, S. Mandla, N. Hu, X. Liu, J. Leijten, Y.-D. Lin, M. A. Hussain, Y. S. Zhang, A. Tamayol and A. Khademhosseini, *Adv. Funct. Mater.*, 2017, **27**, 1605352.
100 Y. J. Tan, X. Tan, W. Y. Yeong and S. B. Tor, *Sci. Rep.*, , DOI:10.1038/srep39140.
101 G. Gao, A. F. Schilling, T. Yonezawa, J. Wang, G. Dai and X. Cui, *Biotechnol. J.*, 2014, **9**, 1304–1311.
102 D. Chimene, C. W. Peak, J. Gentry, J. K. Carrow, L. M. Cross, E. Mondragon, G. B. C. Cardoso, R. Kaunas and A. K. Gaharwar, *ACS Appl. Mater. Interfaces*, , DOI:10.1021/acsami.7b19808.
103 I. T. Ozbolat, H. Chen and Y. Yu, *Robot. Comput.-Integr. Manuf.*, 2014, **30**, 295–304.
104 W. L. Ng, M. H. Goh, W. Y. Yeong and M. W. Naing, *Biomater. Sci.*, 2018, **6**, 562–574.
105 R. Lozano, L. Stevens, B. C. Thompson, K. J. Gilmore, R. Gorkin, E. M. Stewart, M. in het Panhuis, M. Romero-Ortega and G. G. Wallace, *Biomaterials*, 2015, **67**, 264–273.
106 H. W. Ooi, C. Mota, A. T. ten Cate, A. Calore, L. Moroni and M. B. Baker, *Biomacromolecules*, , DOI:10.1021/acs.biomac.8b00696.
107 J. Mayr, C. Saldías and D. Díaz Díaz, *Chem. Soc. Rev.*, 2018, **47**, 1484–1515.
108 A. Vashist, A. Kaushik, A. Vashist, R. D. Jayant, A. Tomitaka, S. Ahmad, Y. K. Gupta and M. Nair, *Biomater. Sci.*, 2016, **4**, 1535–1553.
109 M. Karimi, A. Ghasemi, P. Sahandi Zangabad, R. Rahighi, S. M. Moosavi Basri, H. Mirshekari, M. Amiri, Z. Shafaei Pishabad, A. Aslani, M. Bozorgomid, D. Ghosh, A. Beyzavi, A. Vaseghi, A. R. Aref, L. Haghani, S. Bahrami and M. R. Hamblin, *Chem. Soc. Rev.*, 2016, **45**, 1457–1501.
110 M. J. Webber and R. Langer, *Chem. Soc. Rev.*, 2017, **46**, 6600–6620.
111 J. Nicolas, S. Mura, D. Brambilla, N. Mackiewicz and P. Couvreur, *Chem Soc Rev*, 2013, **42**, 1147–1235.
112 A. Vashist, A. Vashist, Y. K. Gupta and S. Ahmad, *J Mater Chem B*, 2014, **2**, 147–166.

113 C. Murphy, K. Kolan, W. Li, J. Semon, D. Day and M. Leu, *Int. J. Bioprinting*, , DOI:10.18063/IJB.2017.01.005.
114 Y.-W. Chen, Y.-F. Shen, C.-C. Ho, J. Yu, Y.-H. A. Wu, K. Wang, C.-T. Shih and M.-Y. Shie, *Mater. Sci. Eng. C*, 2018, **91**, 679–687.
115 C. Li, A. Faulkner-Jones, A. R. Dun, J. Jin, P. Chen, Y. Xing, Z. Yang, Z. Li, W. Shu, D. Liu and R. R. Duncan, *Angew. Chem. Int. Ed.*, 2015, **54**, 3957–3961.
116 H. Li, Y. J. Tan, K. F. Leong and L. Li, *ACS Appl. Mater. Interfaces*.
117 A. Skardal, D. Mack, E. Kapetanovic, A. Atala, J. D. Jackson, J. Yoo and S. Soker, *STEM CELLS Transl. Med.*, 2012, **1**, 792–802.
118 Y. Li, X. Jiang, L. Li, Z.-N. Chen, G. Gao, R. Yao and W. Sun, *Biofabrication*, 2018, **10**, 044101.
119 F. Xu, S. J. Moon, A. E. Emre, E. S. Turali, Y. S. Song, S. A. Hacking, J. Nagatomi and U. Demirci, *Biofabrication*, 2010, **2**, 014105.
120 S. Rhee, J. L. Puetzer, B. N. Mason, C. A. Reinhart-King and L. J. Bonassar, *ACS Biomater. Sci. Eng.*, 2016, **2**, 1800–1805.
121 A. Matsumoto, J. Chen, A. L. Collette, U.-J. Kim, G. H. Altman, P. Cebe and D. L. Kaplan, *J. Phys. Chem. B*, 2006, **110**, 21630–21638.
122 Z. Zheng, J. Wu, M. Liu, H. Wang, C. Li, M. J. Rodriguez, G. Li, X. Wang and D. L. Kaplan, *Adv. Healthc. Mater.*, 2018, 1701026.
123 M. Tako and S. Nakamura, *Carbohydr. Res.*, 1988, **180**, 277–284.
124 A. D. Graham, S. N. Olof, M. J. Burke, J. P. K. Armstrong, E. A. Mikhailova, J. G. Nicholson, S. J. Box, F. G. Szele, A. W. Perriman and H. Bayley, *Sci. Rep.*, , DOI:10.1038/s41598-017-06358-x.
125 M. Taylor, P. Tomlins and T. Sahota, *Gels*, 2017, **3**, 4.
126 T. Lorson, S. Jaksch, M. M. Lübtow, T. Jüngst, J. Groll, T. Lühmann and R. Luxenhofer, *Biomacromolecules*, 2017, **18**, 2161–2171.
127 F.-Y. Hsieh, H.-H. Lin and S. Hsu, *Biomaterials*, 2015, **71**, 48–57.
128 C.-W. Ou, C.-H. Su, U.-S. Jeng and S. Hsu, *ACS Appl. Mater. Interfaces*, 2014, **6**, 5685–5694.
129 C. J. Bowerman, D. M. Ryan, D. A. Nissan and B. L. Nilsson, *Mol. Biosyst.*, 2009, **5**, 1058.
130 G. Fichman and E. Gazit, *Acta Biomater.*, 2014, **10**, 1671–1682.
131 C. Martin, E. Oyen, J. Mangelschots, M. Bibian, T. Ben Haddou, J. Andrade, J. Gardiner, B. Van Mele, A. Madder, R. Hoogenboom, M. Spetea and S. Ballet, *Medchemcomm*, 2016, **7**, 542–549.
132 B. Raphael, T. Khalil, V. L. Workman, A. Smith, C. P. Brown, C. Streuli, A. Saiani and M. Domingos, *Mater. Lett.*, 2017, **190**, 103–106.
133 A. Biswas, S. Malferrari, D. M. Kalaskar and A. K. Das, *Chem. Commun.*, 2018, **54**, 1778–1781.
134 S. J. Barrow, S. Kasera, M. J. Rowland, J. del Barrio and O. A. Scherman, *Chem. Rev.*, 2015, **115**, 12320–12406.
135 H. Jung, J. S. Park, J. Yeom, N. Selvapalam, K. M. Park, K. Oh, J.-A. Yang, K. H. Park, S. K. Hahn and K. Kim, *Biomacromolecules*, 2014, **15**, 707–714.
136 J. Park, S. J. Lee, S. Chung, J. H. Lee, W. D. Kim, J. Y. Lee and S. A. Park, *Mater. Sci. Eng. C*, 2017, **71**, 678–684.
137 Y. Nishiyama, M. Nakamura, C. Henmi, K. Yamaguchi, S. Mochizuki, H. Nakagawa and K. Takiura, *J. Biomech. Eng.*, 2009, **131**, 035001.
138 K. Christensen, C. Xu, W. Chai, Z. Zhang, J. Fu and Y. Huang, *Biotechnol. Bioeng.*, 2015, **112**, 1047–1055.
139 B. Duan, L. A. Hockaday, K. H. Kang and J. T. Butcher, *J. Biomed. Mater. Res. A*, 2013, **101A**, 1255–1264.
140 Z. Li, S. Huang, Y. Liu, B. Yao, T. Hu, H. Shi, J. Xie and X. Fu, *Sci. Rep.*, , DOI:10.1038/s41598-018-26407-3.
141 D. Nguyen, D. A. Hägg, A. Forsman, J. Ekholm, P. Nimkingratana, C. Brantsing, T. Kalogeropoulos, S. Zaunz, S. Concaro, M. Brittberg, A. Lindahl, P. Gatenholm, A. Enejder and S. Simonsson, *Sci. Rep.*, , DOI:10.1038/s41598-017-00690-y.
142 T. Möller, M. Amoroso, D. Hägg, C. Brantsing, N. Rotter, P. Apelgren, A. Lindahl, L. Kölby and P. Gatenholm, *Plast. Reconstr. Surg. - Glob. Open*, 2017, **5**, e1227.
143 T. Ahlfeld, G. Cidonio, D. Kilian, S. Duin, A. R. Akkineni, J. I. Dawson, S. Yang, A. Lode, R. O. C. Oreffo and M. Gelinsky, *Biofabrication*, 2017, **9**, 034103.
144 X. Yang, Z. Lu, H. Wu, W. Li, L. Zheng and J. Zhao, *Mater. Sci. Eng. C*, 2018, **83**, 195–201.
145 S. Ahn, H. Lee, E. J. Lee and G. Kim, *J. Mater. Chem. B*, 2014, **2**, 2773.
146 G. T. Grant, E. R. Morris, D. A. Rees, P. J. C. Smith and D. Thom, *FEBS Lett.*, 1973, **32**, 195–198.
147 A. Athirasala, A. Tahayeri, G. Thrivikraman, C. M. França, N. Monteiro, V. Tran, J. Ferracane and L. E. Bertassoni, *Biofabrication*, 2018, **10**, 024101.
148 A. Kosik-Kozioł, M. Costantini, T. Bolek, K. Szöke, A. Barbetta, J. Brinchmann and W. Święszkowski, *Biofabrication*, 2017, **9**, 044105.

149 Y. Zhang, Y. Yu, A. Akkouch, A. Dababneh, F. Dolati and I. T. Ozbolat, *Biomater Sci*, 2015, **3**, 134–143.
150 H. Liang, J. He, J. Chang, B. Zhang and D. Li, *Int. J. Bioprinting*, , DOI:10.18063/ijb.v4i1.127.
151 J. M. Grolman, D. Zhang, A. M. Smith, J. S. Moore and K. A. Kilian, *Adv. Mater.*, 2015, **27**, 5512–5517.
152 C. J. Ferris, K. J. Gilmore, S. Beirne, D. McCallum, G. G. Wallace and M. in het Panhuis, *Biomater Sci*, 2013, **1**, 224–230.
153 D. Lee, J. P. Park, M.-Y. Koh, P. Kim, J. Lee, M. Shin and H. Lee, *Biomater. Sci.*, 2018, **6**, 1040–1047.
154 V. Biju, *Chem Soc Rev*, 2014, **43**, 744–764.
155 K. Na, S. Shin, H. Lee, D. Shin, J. Baek, H. Kwak, M. Park, J. Shin and J. Hyun, *J. Ind. Eng. Chem.*, , DOI:10.1016/j.jiec.2017.12.032.
156 J. Yin, M. Yan, Y. Wang, J. Fu and H. Suo, *ACS Appl. Mater. Interfaces*, 2018, **10**, 6849–6857.
157 B. Duan, E. Kapetanovic, L. A. Hockaday and J. T. Butcher, *Acta Biomater.*, 2014, **10**, 1836–1846.
158 D. Qi, S. Wu, M. A. Kuss, W. Shi, S. Chung, P. T. Deegan, A. Kamenskiy, Y. He and B. Duan, *Acta Biomater.*, 2018, **74**, 131–142.
159 S. H. Kim, Y. K. Yeon, J. M. Lee, J. R. Chao, Y. J. Lee, Y. B. Seo, M. T. Sultan, O. J. Lee, J. S. Lee, S. Yoon, I.-S. Hong, G. Khang, S. J. Lee, J. J. Yoo and C. H. Park, *Nat. Commun.*, , DOI:10.1038/s41467-018-03759-y.
160 S. Lin-Gibson, S. Bencherif, J. A. Cooper, S. J. Wetzel, J. M. Antonucci, B. M. Vogel, F. Horkay and N. R. Washburn, *Biomacromolecules*, 2004, **5**, 1280–1287.
161 S. Bertlein, G. Brown, K. S. Lim, T. Jungst, T. Boeck, T. Blunk, J. Tessmar, G. J. Hooper, T. B. F. Woodfield and J. Groll, *Adv. Mater.*, 2017, **29**, 1703404.
162 L. L. Wang, C. B. Highley, Y.-C. Yeh, J. H. Galarraga, S. Uman and J. A. Burdick, *J. Biomed. Mater. Res. A*, 2018, **106**, 865–875.
163 Z. Wang, H. Kumar, Z. Tian, X. Jin, J. F. Holzman, F. Menard and K. Kim, *ACS Appl. Mater. Interfaces*, , DOI:10.1021/acsami.8b06607.
164 C. Di Bella, S. Duchi, C. D. O'Connell, R. Blanchard, C. Augustine, Z. Yue, F. Thompson, C. Richards, S. Beirne, C. Onofrillo, S. H. Bauquier, S. D. Ryan, P. Pivonka, G. G. Wallace and P. F. Choong, *J. Tissue Eng. Regen. Med.*, , DOI:10.1002/term.2476.
165 R. Levato, J. Visser, J. A. Planell, E. Engel, J. Malda and M. A. Mateos-Timoneda, *Biofabrication*, 2014, **6**, 035020.
166 W. Liu, Z. Zhong, N. Hu, Y. Zhou, L. Maggio, A. K. Miri, A. Fragasso, X. Jin, A. Khademhosseini and Y. S. Zhang, *Biofabrication*, 2018, **10**, 024102.
167 W. Jia, P. S. Gungor-Ozkerim, Y. S. Zhang, K. Yue, K. Zhu, W. Liu, Q. Pi, B. Byambaa, M. R. Dokmeci, S. R. Shin and A. Khademhosseini, *Biomaterials*, 2016, **106**, 58–68.
168 X. Cui, K. Breitenkamp, M. Lotz and D. D'Lima, *Biotechnol. Bioeng.*, 2012, **109**, 2357–2368.
169 C. W. Peak, J. Stein, K. A. Gold and A. K. Gaharwar, *Langmuir*, 2018, **34**, 917–925.
170 C. Xu, W. Lee, G. Dai and Y. Hong, *ACS Appl. Mater. Interfaces*, 2018, **10**, 9969–9979.
171 Z. Wang, R. Abdulla, B. Parker, R. Samanipour, S. Ghosh and K. Kim, *Biofabrication*, 2015, **7**, 045009.
172 Y. Ma, Y. Ji, T. Zhong, W. Wan, Q. Yang, A. Li, X. Zhang and M. Lin, *ACS Biomater. Sci. Eng.*, 2017, **3**, 3534–3545.
173 B.-S. Chiou, R. J. English and S. A. Khan, *Macromolecules*, 1996, **29**, 5368–5374.
174 C. E. Hoyle and C. N. Bowman, *Angew. Chem. Int. Ed.*, 2010, **49**, 1540–1573.
175 G.-Z. Li, R. K. Randev, A. H. Soeriyadi, G. Rees, C. Boyer, Z. Tong, T. P. Davis, C. R. Becer and D. M. Haddleton, *Polym. Chem.*, 2010, **1**, 1196.
176 L. Lecamp, F. Houllier, B. Youssef and C. Bunel, *Polymer*, 2001, **42**, 2727–2736.
177 A. Skardal, J. Zhang and G. D. Prestwich, *Biomaterials*, 2010, **31**, 6173–6181.
178 M. Yan, P. L. Lewis and R. N. Shah, *Biofabrication*, 2018, **10**, 035010.
179 Z. Du, N. Li, Y. Hua, Y. Shi, C. Bao, H. Zhang, Y. Yang, Q. Lin and L. Zhu, *Chem. Commun.*, 2017, **53**, 13023–13026.
180 X. Dai, C. Ma, Q. Lan and T. Xu, *Biofabrication*, 2016, **8**, 045005.
181 K. Arai, Y. Tsukamoto, H. Yoshida, H. Sanae, T. A. Mir, S. Sakai, T. Yoshida, M. Okabe, T. Nikaido, M. Taya and others, *Int. J. Bioprinting*.
182 Q. Wei, W. Xu, Q. Zhang, S. Zhang, L. Cheng and Q. Wang, *J Mater Chem B*, 2017, **5**, 5092–5095.
183 X. Cui and T. Boland, *Biomaterials*, 2009, **30**, 6221–6227.
184 N. Law, B. Doney, H. Glover, Y. Qin, Z. M. Aman, T. B. Sercombe, L. J. Liew, R. J. Dilley and B. J. Doyle, *J. Mech. Behav. Biomed. Mater.*, 2018, **77**, 389–399.
185 Y. Loo, A. Lakshmanan, M. Ni, L. L. Toh, S. Wang and C. A. E. Hauser, *Nano Lett.*, 2015, **15**, 6919–6925.
186 K. Zhu, N. Chen, X. Liu, X. Mu, W. Zhang, C. Wang and Y. S. Zhang, *Macromol. Biosci.*, 2018, 1800127.
187 K. Ling, G. Huang, J. Liu, X. Zhang, Y. Ma, T. Lu and F. Xu, *Engineering*, 2015, **1**, 269–274.